Botanical Journal of the Linnean Society, 2022, **200**, 491–523. With 10 figures.

New data for palaeoclimatic reconstructions in the upper/middle Uruguay River Basin: caesalpinioid Fabaceae woods in the Late Pleistocene

R. SOLEDAD RAMOS[1,*], MARIANA BREA[1,2,3], DANIELA M. KRÖHLING[4] and SILVINA A. CONTRERAS[5]

[1]*Laboratorio de Paleobotánica, Centro de Investigación Científica y de Transferencia Tecnológica a la Producción, CICYTTP (CONICET-Prov. ER-UADER), Diamante, Entre Ríos, Argentina*
[2]*Universidad Autónoma de Entre Ríos, Facultad de Ciencia y Tecnología, Sede Diamante, Diamante, Entre Ríos, Argentina*
[3]*Univerisdad Nacional de La Plata, cátedra de Paleobotánica, Facultad de Ciencias Naturales y Museo, La Plata, Argentina*
[4]*CONICET and Universidad Nacional del Litoral, Facultad de Ingeniería y Ciencias Hídricas, Santa Fe, Argentina*
[5]*Laboratorio de Evolución de Vertebrados y Ambientes Cenozoicos. Centro de Ecología Aplicada del Litoral (CONICET-UNNE), Corrientes, Argentina*

Received 17 August 2021; revised 17 February 2022; accepted for publication 28 February 2022

The El Palmar Formation is the principal unit deposited during the Late Pleistocene by the Uruguay River in eastern Entre Ríos province, Argentina and north-western Uruguay. The Arroyo Yuquerí fossiliferous locality (*c*. 31°36′ S, 58°06′ W), part of the El Palmar Formation, is one of the richest sites in fossil woods. This article describes and determines 11 fossil woods, including seven new species closely related to modern *Parapiptadenia*, *Microlobius*, *Anadenanthera*, *Pseudopiptadenia* (Mimoseae, Fabaceae) and *Chloroleucon*, *Enterolobium* and *Cedrelinga* (Ingeae, Fabaceae). Coexistence approach, nearest living relatives (NLR) methods and mesomorphic and vulnerability indices were used to determine palaeoclimatic conditions. Comparisons of NLR of fossil woods, coupled with other previously identified taxa, suggest that a mature and evergreen woodland was present in the middle Uruguay River Basin during some Pleistocene events (MIS 5a and MIS7, according to absolute datings of the fossiliferous sedimentary unit). This caesalpinoid legume woodland was shaped by an environment with abundant humidity, and the structure of the water conduction system in the studied species was efficient. Finally, the results indicate a more humid and warmer climate than at present in the study area.

ADDITIONAL KEYWORDS: Carlquist's indices – coexistence approach – fossil wood – Quaternary – South America.

INTRODUCTION

The evolution of the large La Plata River System, which integrates the Paraná, Paraguay and Uruguay River Basins, had a significant impact on landscape evolution in the mid-latitudes of South America since it has acted as a natural barrier for many terrestrial organisms and as a dispersal route for others (Veroslavsky & Ubilla, 2007). Recent studies on geomorphology and Quaternary stratigraphy (Iriondo & Kröhling, 2008; Kröhling *et al.*, 2014) demonstrate that the Uruguay River Basin experienced climatic and palaeoenvironmental changes during the Quaternary. Hence, plant and animal populations were forced to migrate and adapt to these environmental changes (Lowe & Walker, 2014).

A few comprehensive works have inferred the climatic conditions and the taxonomy of the woody species that lived in the Uruguay River Basin during the Pleistocene and Holocene (Brea, Zucol & Patterer,

*Corresponding author. E-mail: soledadramos.sr@gmail.com

2010; Ramos, Brea & Kröhling, 2012, 2014, 2017a, b). In this work, we add new data for palaeoclimatic reconstructions in the upper/middle Uruguay River Basin based on the research of seven new fossil woods of Fabaceae from the Uruguay River Basin, using anatomical and ecological traits.

The Uruguay River is one of the largest rivers in South America, with a basin that covers *c*. 365 000 km² (south-eastern Brazil, north-eastern Argentina and western Uruguay) and links areas with a present tropical-subtropical humid climate (the upper basin) with areas of temperate climates (the lower basin, near its mouth in the La Plata River Estuary) (Iriondo & Kröhling, 2008).

The upper Uruguay River Basin (Fig. 1; from 26°30´ to 28°30´ S), developed on the Late Cretaceous Paraná Basaltic Plateau (Kröhling *et al.*, 2014), currently covered by subtropical forest. It is included in the macroecological domain of the *Araucaria* Juss. Plateau by Ab'Sáber (2000), and characterized by medium elevation plateaus, 800–1300 m a.s.l. These subtropical ecosystems developed after the mid-Cenozoic.

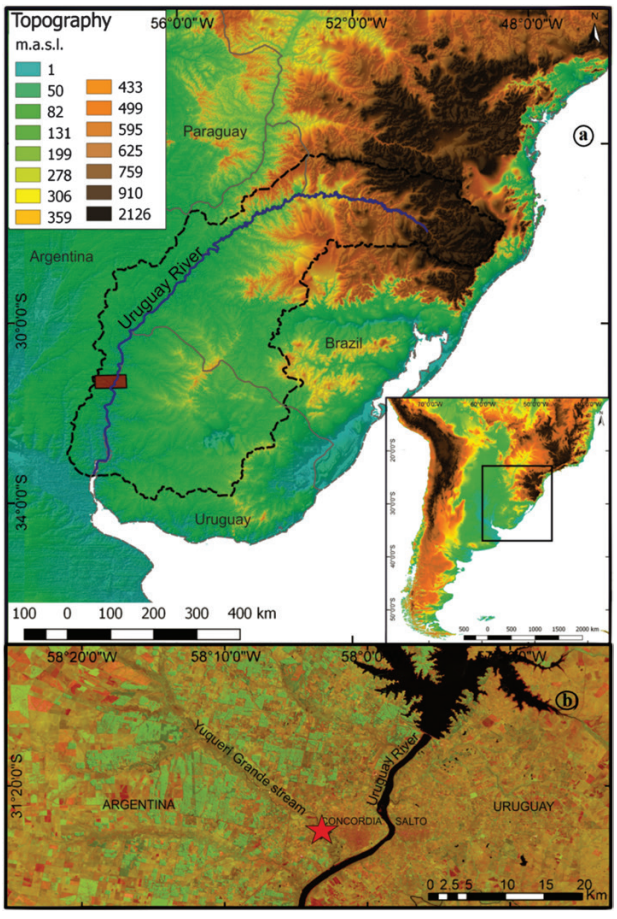

Figure 1. A, The Uruguay River Basin represented in a shaded relief SRTM DEM map. The location of the study area is indicated by the red rectangle. Inset is a GTOPO30 DEM view. B, Landsat-8 image (NASA, with a combination of B6, B5, B4 bands in Google Earth Engine©) of the study area. The fossiliferous locality is marked by the red star.

The middle fluvial basin (from 28°30´ to 32°30´ S) is characterized by Quaternary sedimentary units, mainly of fluvial and paludal origin (Iriondo & Kröhling, 2008). A subtropical/temperate steppe (Pampean phytogeographic province), with areas of temperate-humid savannahs with isolated trees (Espinal phytogeographic province), and gallery woodlands (Paranaense phytogeographic province) predominate in this sector of the basin (Cabrera, 1976; Oyarzabal, Clavijo & Oakley, 2018; Arana *et al.*, 2021).

Relictual populations of *Butia yatay* (Mart.) Becc. are preserved in El Palmar National Park in the middle Uruguay Basin (31° 55´ S, 58° 16´ W, 8500 ha) in Argentina. The El Palmar Formation (Iriondo, 1980; Iriondo & Kröhling, 2008) is the main unit deposited by the Uruguay River in the middle basin (28/33°S and 58°W; eastern Entre Ríos province, Argentina and north-western Uruguay) during the Late Pleistocene (Fig. 1).

The Arroyo Yuquerí fossiliferous locality (Fig. 1) is one of the richest sites in fossil woods represented by *Palmoxylon yuqueriensis* Lutz (Arecaceae), *Bastardiopsis paleodensiflora* Ramos, Brea & Kröhling (Malvaceae), *Gossweilerodendroxylon palmariensis* Ramos, Brea & Kröhling (Fabaceae) and species related to Anacardiaceae (Lutz, 1979; Ramos, 2015; Ramos *et al.*, 2017a, b).

Fabaceae are considered to be one of the most diverse families due to the great morphological, physiological and ecological variability of the species. They are cosmopolitan in distribution, and they are significant elements in lowland forests in South America (LPWG, 2017). Legumes are among the most numerous species in the riverside forests of the Uruguay River and its tributaries (Guido & López Mársico, 2011; González & Cadenazzi, 2015).

Caesalpinioideae comprise 148 genera and *c*. 4400 species (LPWG, 2017) and are a common pantropical subfamily of humid and dry regions, with some species living in temperate zones and rare species living in cold environments. Caesalpinioideae are monophyletic and include the *Piptadenia* Benth. group, which will be further discussed in this work (Lewis *et al.*, 2005; Yahana *et al.* 2013). In South America, Caesalpinioideae occur in tropical and subtropical areas, from rain forests, evergreen or deciduous forests, to savannas, semi-deserts and high mountains (Ulibarri, 2008; Zuloaga *et al.*, 2008).

The fossil records of Caesalpinioideae in South America are extensive and consist mainly of wood, pollen, leaf impressions, fruits and seeds (Pujana, Martínez & Brea, 2011; Ramos, Brea & Pardo, 2014;

Benicio *et al.*, 2016; Woodcock, Meyer & Prado, 2017). Many of these records are from Argentina, with records for the mimosoid clade being the most abundant (*c.* 25 spp.), and genera include *Mimosoxylon* Felix, *Tetrapleuroxylon* Felix, *Paracacioxylon* Menendez, *Gleditsioxylon* Prakash & Barghoorn, *Piptadenioxylon* Suguio & Mussa, *Menendoxylon* Lutz, *Anadenantheroxylon* Brea, Aceñolaza & Zucol, *Prosopisinoxylon* Martínez, *Microlobiusxylon* Franco & Brea, *Paraalbizioxylon* Martínez, *Abaremaxylon* Moya & Brea, *Cylicodiscuxylon* Moya & Brea and a species of *Parkinsonia* Plum. ex L. (Pujana *et al.*, 2011; Ramos *et al.*, 2012, 2020; Franco & Brea, 2013; Martinez, 2014; Moya & Brea, 2015; Martínez & Crisafulli, 2018; Baez & Crisafulli, 2020; Mautino & Garralla, 2021 etc.). The purpose of this work is: (1) to describe the anatomy of the fossil woods recovered from the Arroyo Yuquerí fossiliferous locality (El Palmar Formation), (2) to identify taxonomic affinities and (3) to infer palaeoclimatic conditions associated with the Uruguay fluvial valley during some episodes of the Upper Quaternary using diverse methodologies, such as ecological anatomical characters, mesomorphy and vulnerability indices (MI and VI, respectively) and nearest living relative (NLR) and coexistence approach (CA) methods.

Study area, palaeobotanical and geological setting

The El Palmar Formation was formally defined by Iriondo (1980) along quarry outcrops and boreholes in the area of El Palmar National Park (Entre Ríos province, Argentina). This unit is composed of red to yellowish-brown sandy strata with interbedded gravels outcropping at the upper fluvial terrace surface of the Uruguay River with a width of 4–15 km on its right margin. This sedimentary unit (10–17 m thick) covers Cretaceous rocks. Locally a Late Holocene aeolian sandy unit unconformably overlies the El Palmar Formation (see Patterer, Kröhling & Zucol, 2020). The provenance sources of the sediments composing this unit (mainly sands and gravels) are Mesozoic rocks (sandstones and basalts) of the upper Uruguay River Basin (Iriondo & Kröhling, 2008). The main stratigraphic characteristics of the El Palmar Formation are presented in Iriondo & Kröhling (2008) and Patterer *et al.* (2020). Channel lag gravels, longitudinal gravel bars and low-angle cross-bedded sand bars represent channel deposits. Laminated fine sands to clayey silts constitute abandoned channel infillings and overbank deposits. The unit contains lenticular strata, mainly composed of fine to medium and well-rounded siliceous pebbles and medium to coarse well-rounded gravels in a sandy/clayey matrix, with planar bedding, indicating high fluvial transport energy and high-river discharges. The sedimentary facies association and its architecture represent a large depositional fluvial system (bedload river). The sedimentary data along a north–south transect of the El Palmar Formation depositional area indicate a downstream decrease in the gravel/sand ratio and in the gravel sizes. The unit was cemented differentially by silica and iron oxides (Iriondo & Kröhling, 2008; Kröhling, 2009; Patterer *et al.*, 2020). On the left margin of the Uruguay River in its middle basin (Uruguay), Bossi (1969) defined the Salto Formation, a unit that was correlated by Iriondo & Kröhling (2008) with the El Palmar Formation.

The upper part of the El Palmar Formation was dated by thermoluminescence (TL), yielding ages between *c.* 80 and 88 kya BP (Iriondo & Kröhling, 2008; Kröhling, 2009), interpreted by these authors as representative of the warm substage marine isotope stage 5a (MIS 5a). Recently, an optically stimulated luminescence dating of sediments from the upper part of the El Palmar Formation in the type area (El Palmar National Park) yielded an age of 184 491 ± 13 946 years BP (Lab Code L0090, Laboratório de Espectrometria Gama e Luminescência, USP, Brazil). These data would extend the age of the El Palmar Formation to the penultimate interglacial (MIS 7; Middle Pleistocene) (Ramos, 2015; Ramos *et al.*, 2017a). These are the only absolute datings of the El Palmar Formation and are of great importance for environmental Quaternary reconstructions of the large fluvial environments of South America.

The El Palmar Formation provided important micro- and macrofossil plant records (Lutz, 1979, 1980, 1984, 1986; Brea, 1998, 1999; Brea & Zucol, 2001a, b, 2011; Brea, Aceñolaza & Zucol, 2001; Brea *et al.*, 2010; Zucol *et al.*, 2005; Ramos *et al.*, 2012, 2014, 2015, 2017a, b; Patterer, Zucol & Brea, 2014). This unit is rich and diverse in fossil wood. In the doctoral thesis of the first author, 56 fossil woods were studied, 28 corresponding to Fabaceae, of which 24 belong to Caesalpinioideae (Ramos *et al.*, 2012, 2014, 2017a, b; Ramos, 2015). In addition, ten fossil specimens related to Fabaceae published by other authors were identified (Lutz, 1979, 1991; Brea, 1999; Brea *et al.*, 2010). Thus, legumes represent 58% of the total number of wood samples. Vertebrate palaeontological data belonging to the Lujanian South American Land Mammal Age (Late Pleistocene-Early Holocene) were also recorded for this unit (Tonni, 1987; Ferrero *et al.*, 2007, 2019; Brandoni, Ferrero & Brunetto, 2010).

The Arroyo Yuquerí fossiliferous locality is placed near the mouth of the Yuquerí Grande Stream in the Uruguay River, at the old railway bridge close to the city of Concordia in Entre Ríos province, Argentina (*c.* 31°36′ S, 58°06′ W) (Fig. 1). The El Palmar Formation dominates the fossiliferous area, covering basaltic

rocks. There, the stratigraphic profiles are deeply eroded and the fossil woods are exposed over the Yuquerí floodplain. In the present days, this region is under a subtropical humid climate, with rainfalls between 1200 and 1300 mm/year, and mean annual temperatures of 18–19 °C.

MATERIAL AND METHODS

Fossil wood preparation and analysis

The fossil woods described here are silicified with good preservation and were collected by Cristina Vassallo de Cettour and Silvia Cettour (Head of Department of the Museo de Antropología y Ciencias Naturales, Concordia, Entre Ríos, Argentina). Standard petrographic sections (*c.* 20–40 µm thick) were obtained in transverse (TS), tangential longitudinal (TLS) and radial longitudinal (RLS) orientations for each of the studied specimens. Quantitative characters were based on at least 25 measurements. The numbers in brackets indicate the minimum and maximum values. The material was studied with a Nikon Eclipse E200 light microscope, and photomicrographs were taken with a Nikon Coolpix S4 digital camera.

InsideWood (IWD) is a database with > 9400 descriptions of fossil and modern woody dicots and conifers, and it represents > 10 000 species (Wheeler, Gasson & Baas, 2020). It is also an important reservoir of descriptions of modern legumes from South America encoded with their qualitative and quantitative features. The searches in IWD were completed with key literature, such as Cozzo (1951), Banks & Gasson (2000), Evans, Gasson & Lewis (2006), Gasson, Trafford & Matthews (2003), Metcalfe & Chalk (1950), Tortorelli (1956), Wheeler (2011) etc., to obtain the taxonomic identification of the samples under study. After relating and taxonomically identifying the fossil woods with extant species, they were compared with fossil legume species mainly from South America, considering articles from IWD (2004-onwards) and by Ramanujam (1960), Müller-Stoll & Mädel (1967), Gregory, Poole & Wheeler (2009), Shukla, Mehrotra & Guleria, (2013), Pujana *et al.* (2011, 2014) etc. (Table 1). The anatomical terms used in this paper follow the recommendations of the IAWA List of Microscopic Features for Hardwood Identification (IAWA Committee, 1989).

The systematic and taxonomic assignment of the Fabaceae followed the classification of APG IV (2016) and LPWG (2017). The World Flora Online (WFO, 2020) and the Index Nominum Genericorum (Farr & Zijlstra, 1996) were used to check the taxonomic names.

The repository of the fossil specimens and microscope slides is the Laboratorio de Paleobotánica, CICYTTP (CONICET-Prov. ER-UADER), Diamante, Argentina. The acronym used for woods specimens was CIDPALBO-MEG, and CIDPALBO-MIC for slides.

Eleven fossil woods were described for this study. Dimensions of the specimens are as follows: CIDPALBO-MEG 119 is 11 cm long and 9 cm in diameter; CIDPALBO-MEG 123 is 15 cm long and 6 cm in diameter; CIDPALBO-MEG 120 and 122 are 39–30 cm long and 6–8 cm in diameter; CIDPALBO-MEG 127 and 129 are 8–12 cm long and 7–10 cm in diameter, CIDPALBO-MEG 128 is 15 cm long and 11 cm in diameter, CIDPALBO-MEG 132 is 25 cm long and 8 cm in diameter, CIDPALBO-MEG 137 is 20 cm long and 11 cm in diameter; and CIDPALBO-MEG 141 and 143 are 8–12 cm long and 5–8 cm in diameter.

The nearest living relative and coexistence approaches

The NLR method of Mosbrugger (1999), based on eco-anatomical analysis and climatic requirements of a set of taxa, was used to obtain palaeoenvironmental data. This method assumes that Pleistocene plant taxa have climatic requirements similar to those of their NLRs. The CA method was used for estimating climate parameters (Mosbrugger & Utescher, 1997; Utescher *et al.*, 2014). The CA aims to find for a given fossil flora a climate parameter or the climatic interval in which all the NLRs of the fossil flora can coexist. The terms tropical, subtropical and temperate are used in this article to indicate broad geographical/macroclimatic zones. Therefore, tropical implies non-seasonal, equable warm and humid climates, whereas temperate implies markedly seasonal climates, with seasonality in temperature and/or water availability (*sensu* Wheeler & Baas, 1993).

The resolution of the resulting coexistence intervals increases with the number of taxa included in the analysis and are relatively high in floras with ten or more taxa for which climate parameters are known. The percentage of NLR coexisting in the resulting climate intervals is considered as the measure of the significance of the results obtained. This analysis includes other fossil species already known from the Arroyo Yuquerí fossiliferous locality, mentioned in the Introduction section.

Each taxon must have its climatic data requirements or tolerance data derived from its modern distribution area, assuming that extant taxa live in a place within their minimum and maximum tolerance of climatic parameters (Cozzo, 1951; Metcalfe & Chalk, 1950; Tortorelli, 1956; Tomazello Filho, Peres Chimelo & Vieitez Garcia, 1983; Costa *et al.*, 1997; Miller & Detienne, 2001; Evans *et al.*, 2006; León, 2008; Lima, Oliveira & Rodrigues, 2009; Arambarri *et al.*, 2012).

Table 1. Comparison of the fossil woods from the El Palmar Formation with the related fossil genera, and anatomical wood data of the studied fossils used to calculate the vulnerability index (VI) and mesomorphy index (MI)

Fossils	Growth rings	Vessels				Pits	Fibres	Axial parenchyma	Rays			PC	SE	VI	MI
		Solitary	TD µm	mm^2	Length µm	D µm	Septate		Type	Height (cells)	Width cells				
Parapiptadenioxylon pararigida (this work)	Dp	68%	106	9	195	7	No	V, A, <C; M	Ho	9 (4–12)	1 (1 – 3)	A	≈ R	**12**	**2296**
Pseudopiptadenioxylon uniseriatum(this work)	Dpf	77%	91	12	198	7	No	V, >A, <C; M	Ho	13 (4–23)	1	A	A	**7**	**1501**
Microlobiusxylon parafoetidus(this work)	Dp	84%	86	12	225	9	No-Yes?	V, A, C; M, D	Ho	16 (4–27)	1	PS	A	**7**	**1612**
Anadenantheroxylon kurupaum(this work)	Dpf	66%	108	11	256	7	No	>V, A, C; M	Ho	14 (4–24)	2 (1–3)	PS	A	**10**	**2513**
Cedrelinga paleocatenaeformis(this work)	LD	72%	133	8	260	9	No	<V, A, C; M, D	Ho	15 (2–40)	1	?	A	**17**	**4322**
Chloroleucoxylon yukeriense(this work)	D	80%	75	10	170	8	No	V, A, C; M	Ho	12 (3–26)	1	?	A	**8**	**1275**
Enterolobiumoxylon vassalloae(this work)	D	73%	133	7	312	10	No-Yes?	V, A, C; M, D	Ho	15 (2 – 38)	2 (1 – 3)	A	A	**19**	**5928**
Menendoxylon	D	60%	≤200	12–30	≤300	3 – 10	No	V, A, C	Ho	8 – 39	1–3	--	≈ R		
Anadenantheroxylon	D	60%	106	15–24	192	11 (5 – 34)	No	V, A, C	Ho	7 – 25	2 (1, 3)	PS	A		
Piptadenioxylon	D	90%	40 – 100	15–21	≤350	≤7	No	V, A, C	Ho	?	2, 3 (1)	?	≈ R		
Microlobiusxylon	D	80%	40 – 115	18 – 28	≤350	≤7	No	>V, A, C	Ho	4 – 35	1–2	PS	A		
Cylicodiscuxylon	Df	53%	124	6	219	7	No	V, A, C	Ho	11 (6 – 19)	2 (1 – 3)	PS	A		
Abaremaxylon	Df	84%	108	10	601	6	No	V, U, A, C	Ho	8 (4 – 13)	1	PS	A		
Enterolobiumoxylon	A	60 %	176	4	327	8	No	A, C, D	Ho	14	1 (1 – 3)	PS	A		
Brachystegioxylon	D	?	≤200	≤20	≤350	4 – 6	¿	V, A, C, M	Ho	?	1 – 3	PS	A		
Albizzinium	D	?	80 – 200	20	150 – 450	6 – 8	Yes	V, A, C, M, D	Ho	?	2 – 10	PS	A		
Albizzioxylon	D	?	115 – 280	3 – 6	≤350	4 – 6	Yes	V, A, C, M	Ho	3 – 25	1 – 10	A	A		
Dalbergioxylon	I	?	100 – 200	3 – 12	≤350	6 – 9	No	V, A, M, B	Ho, He	4 – 12	1 – 3	PS, R	P, V, R		

Mesomorphy (MI) and vulnerability (VI) values are in bold in the body of the table.
Key to abbreviations used:
- Growth rings: D = distinct, LD = slightly distinct, Dp = distinct marked by marginal parenchyma, Dpf = distinct marked by marginal parenchyma and fibres, Df = distinct marked by fibres
- Vessels: TD = tangential diameter
- Ray type: Ho = homocellular, He = heterocellular
- SE = Storied structure: A = absent, P = present, R = in rays
- Axial parenchyma type: D = diffuse, A = aliform, V = vasicentric, C = confluent, M = marginal, U = unilateral
- PC = Prismatic crystals: A = not seen, F = in fibres, PS = in chambered axial parenchyma cells
- Vulnerability index (VI) and mesomorphy index (MI)

Subsequently, a diagram with the parameters of all the NLRs is generated, and the CA is extracted. These parameters of the association are obtained as a tolerance range (Jordan, 1997; Mosbrugger, 1999). The advantage of this method is that it is not necessary to find modern flora comparable to the identified fossil flora, as it allows building scenarios through the specific interaction of the taxa set (Mosbrugger & Utescher, 1997; Utescher *et al.*, 2014). A detailed description and discussion of the method can be found in Mosbrugger (1999).

In this study, the climatic parameters estimated are mean annual temperature (MAT), the temperature of the coldest month (MiT), the temperature of the warmest month (MaT), mean annual precipitation (MAP) and mean maximum and minimum annual precipitation of the area where the NLRs live (MaP and MiP, respectively).

Vulnerability and mesomorphy indices

The vulnerability index (VI) is used as an indicator of hydraulic conductivity, and it is indicative of the sensitivity to the risk of embolisms. Low VI value indicates woods with a greater capacity for withstanding water stress or freezing. High VI values indicate woods with wide/few vessels and efficient water conductors. The mesomorphy index (MI) is an equation relating to vulnerability multiplied by vessel element length. A high value in the MI indicates efficient wood structure and development in an environment with no water limitations. For further details about this method, refer to Carlquist (2001) and Ramos (2014).

$$VI = MDT_{vessels}/V \text{ per mm}^2 \text{ (Mean Diameter Tangential vessel/ Vessels per mm}^2\text{)}$$

$$MI = VI * Length_{vessel} \text{ (Vulnerability} * \text{Mean Vessel element length)}$$

Statistical analyses

Infostat software (Infostat, 2016) was used to corroborate the accuracy of the systematic placement or affinity between extant and fossil taxa of Mimoseae and Ingeae.

Twenty-four anatomical features of fossil species were used for the statistical analyses. A principal component analysis (PCA) was performed to evaluate how the quantitative traits were related (see Appendix), and qualitative features were analysed in a principal coordinate analysis using a simple matching similarity index. Qualitative and quantitative features were studied together using a generalized pro-cruster analysis (GPA) to obtain a consensus (Gower, 1975). As an additional analysis, species of Caesalpinioideae with low VI values living in seasonal environments and species with high VI values living in humid environments were randomly incorporated. Finally, two random species from a different subfamily from that of the fossils were used as the outgroup. The species selected for this analysis were: *Albizia inundata* (Mart.) Barneby & Grimes (Baldin & Marchiori, 2014), *Inga alba* (Sw.) Willd (León, 2008), *Mimosa polyantha* Benth (Montalo-Arias, Camargo & Grether, 2016), *Prosopis kuntzei* L. and *P. alpaca* Phil. (Castro, 1994; Villagra & Roig, 1997), *Samanea saman* (Jacq.) Merr [synonym: *Pithecellobium saman* (Jacq.) Benth.] (Silva, Blanco & Lindorf, 1989), *Prosopis vinalillo* Stuck. (Bolzón de Muñiz, Nisgoski & Lomelí-Ramírez, 2010), *Vachellia caven* Mol. Seigler & Ebinger (Cozzo, 1951) and *Zygia longifolia* (Willd.) Britton & Rose (Evans *et al.* 2006). The outgroup consisted of *Cadia purpurea* (Piccioli) Aiton (Sophoreae; Stepanovaab *et al.* 2013) and *Geoffroea decorticans* Burkart (Dalbergieae; Gimenez, 2009).

SYSTEMATIC PALAEOBOTANY

DESCRIPTION AND SYSTEMATICS OF THE WOOD TYPES

Family Fabaceae
Subfamily Caesalpinioideae
Tribe Mimoseae
Genus *Parapiptadenioxylon* gen. nov. Ramos, Brea, Kröhling & Contreras

Parapiptadenioxylon pararigida gen. nov. & sp. nov. Ramos, Brea, Kröhling & Contreras (Fig. 2A–K).

Etymology: Parapiptadenioxylon refers to its affinity with *Parapiptadenia* Brenan. The specific name *pararigida* refers to its affinity with the extant species *Parapiptadenia rigida* (Benth.) Brenan.

Genus and species diagnosis. Growth ring boundary. Vessels solitary and radial multiples of two to four elements. Intervessel pits small to medium. Axial parenchyma paratracheal vasicentric, aliform and confluent; axial parenchyma apotracheal marginal and diffuse. Rays one to three cells wide (mostly uniseriate), all ray cells procumbent. Fibres non-septate. Parenchyma strand of two to eight cells.

Holotype: CIDPALBO-MEG 120—CIDPALBO-MIC 1543 (three microscopic slides).

Paratype: CIDPALBO-MEG 122—CIDPALBO-MIC 1545 (three microscopic slides).

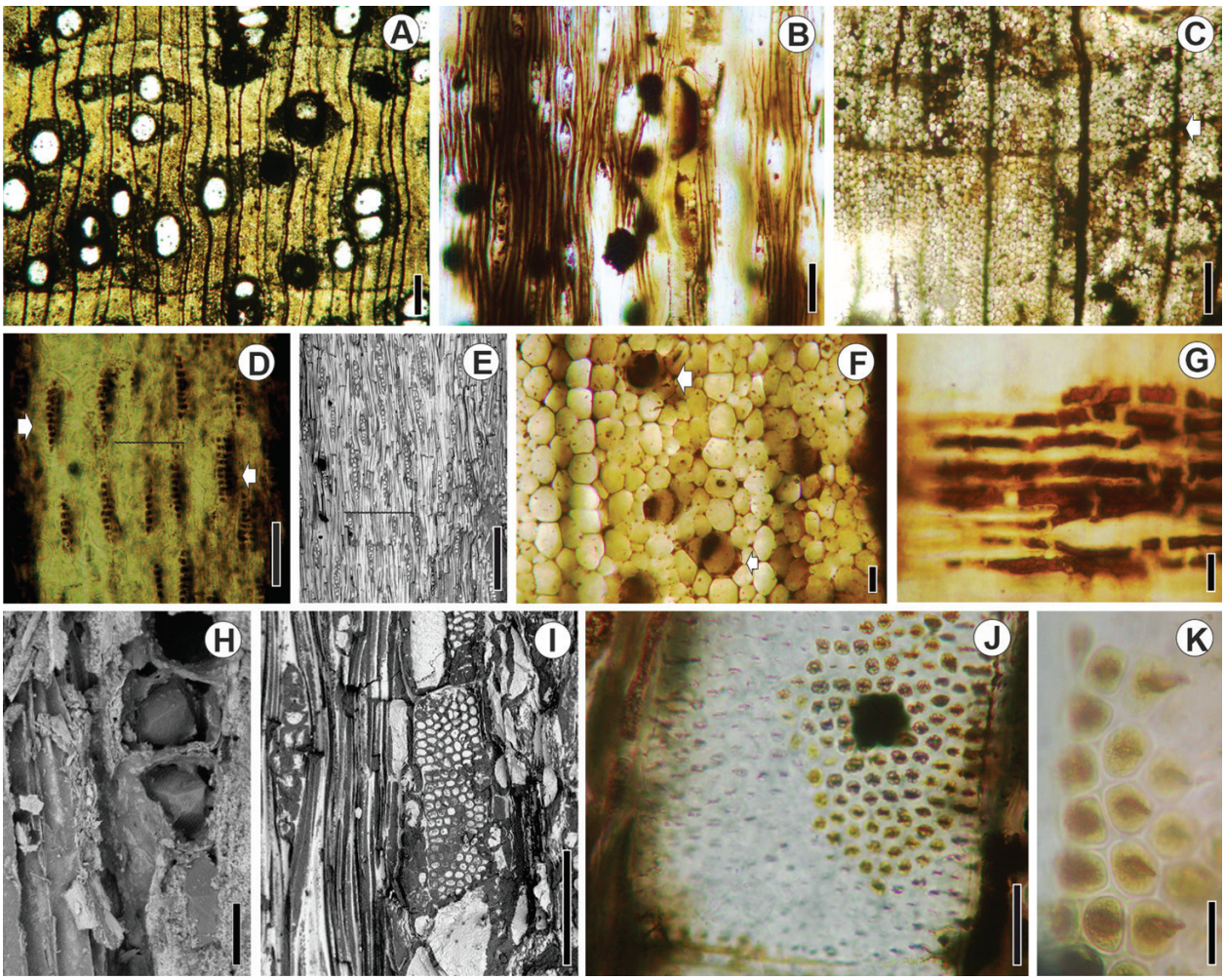

Figure 2. *Parapiptadenioxylon pararigida* sp. nov. Ramos Brea Kröhling & Contreras. (Material examined CIDPALBO-MEG 120–CIDPALBO-MIC 1543: A, C, D, F, J, H, K; CIDPALBO-MEG 122-CIDPALBO-MIC 1545: B, E, G, I). A, Transverse section (TS), general view, wood diffuse-porous, axial parenchyma vasicentric, 200 µm. B, Tangential longitudinal section (TLS), detail of ray with width one to three cells and stand parenchyma, 100 µm. C, TS general view of fibres, axial parenchyma and growth rings, 100 µm. D, TLS general view showing partially storied rays, 100 µm. E, TLS general view showing rays partial storied [scanning electron microscopy (SEM)], 300 µm. F, TS diffuse axial parenchyma, 20 µm. G, Radial longitudinal section (RLS), general view showing homocellular rays composed of procumbent cells, 20 µm. H, TLS, prismatic crystals in rays (SEM), 10 µm. I, TLS, vessel element and alternate intervessel pits (SEM), 100 µm. J, RLS detail of medium, bordered, alternate, circular and vestured intervessel pits, 20 µm. K, TLS, detail of alternate and vestured intervessel pits, 10 µm.

Repository: Laboratorio de Paleobotánica, CICYTTP (CONICET-Prov. ER-UADER).

Stratigraphic unit: El Palmar Formation, Late Pleistocene.

Locality: Arroyo Yuquerí, Entre Ríos province, Argentina.

Search criteria InsideWood: 13p 22p 26p 29p 30p 42p 47p 52p 66p 79p 80p 83p 89p 97p 104p 115p 188p (IAWA features).

Description

Growth ring boundary, demarcated by narrow axial parenchyma marginal. Wood diffuse-porous. Vessels solitary (68%) and in radial multiples of two elements (19%) and three elements (10%), rarely of four elements (3%), circular to oval in outline (Fig. 2A), tangential diameter 106 (56–190) µm, radial diameter 92 (31–187) µm, walls 10 (7–15) µm thick (Fig. 2A, I), nine (seven to 11) vessels per square mm, vessel element 195 (132–250) µm are short; perforation plates simple; intervessel pits alternate, vestured, diameter

7 (6–9) µm (Fig. 2I–K); vessel-ray parenchyma pits similar to intervessel pits, small, diameter ≤ 6 µm. Dark deposits occur in vessels (Fig. 2A).

Axial parenchyma paratracheal vasicentric to aliform and confluent (Fig. 2A), also axial parenchyma apotracheal marginal and rare diffuse (Fig. 2C, F). Axial parenchyma strands of two to ten cells (Fig. 2B).

Rays ten (eight to 13)/mm, uniseriate (85%), two (9%) and three cells wide (6%), 25 (13–35) µm in width, ray height 154 (64–228) µm or nine (three to 16) cells, all ray cells procumbent (Fig. 2B, D, E, G). Rays irregularly storied (Fig. 2D, E). Prismatic crystals in ray cells (Fig. 2H).

Fibres non-septate, polygonal, angular and oval in outline; diameter 12 (6–18) µm, and thick-walled (Fig. 2B, I).

Affinity and comparisons

The presence of vestured intervessel pits and vessel elements with simple perforation plate are the synapomorphies that allow the placement of this specimen in Fabales (Judd *et al.*, 1999). However, the predominance of homocellular rays composed exclusively of procumbent cells, axial parenchyma paratracheal and alternate and vestured intervessel pits is characteristic of the mimosoid clade of Fabaceae subfamily Caesalpinioideae (Metcalfe & Chalk, 1950; Baretta-Kuipers, 1981; Höhn, 1999; Herendeen, 2000; Gasson *et al.*, 2003; Espinoza de Pernía & Melandri, 2006). Vestured intervessel pits are absent in the newly recognized subfamilies Duparquetioideae, Cercidoideae and most genera of Dialioideae, whereas they are present in Papilionoideae, Detarioideae and Caesalpinioideae (Quirk & Miller, 1985; Herendeen, 2000; Bruneau *et al.*, 2008; LPWG, 2017). It is also usual to observe diffuse parenchyma strands, which usually contain ten or more chambered crystals (Metcalfe & Chalk, 1950; Müller-Stoll & Mädel, 1967; Wheeler & Baas, 1992; Evans *et al.*, 2006).

In general, Caesalpinioideae have diffuse-porous wood without a predominant vessel arrangement, paratracheal parenchyma from aliform to confluent and often banded, uni- or bi-triseriate and occasionally multiseriate rays that are homocellular composed of procumbent cells, and the absence of storied elements (Metcalfe & Chalk, 1950; Cozzo, 1951; Baretta-Kuipers, 1981; Wheeler & Baas, 1992; Marchiori & de Muñiz, 1996; Gasson *et al.*, 2003; Evans *et al.*, 2006; da Silva *et al.*, 2011; Ramos *et al.*, 2017b).

Mimosa L., *Anadenanthera* Speg., *Parapiptadenia*, *Piptadenia*, *Pseudopiptadenia* Rauschert, *Stryphnodendron* Mart., *Adenopodía* C.Presl. and *Microlobius* C.Presl. are the genera of the *Piptadenia* group (Mimoseae, Caesalpinioideae). Members of this group usually have homocellular rays one to five cells wide, scarcer heterocellular rays, axial parenchyma narrow bands and non-septate fibres (Cozzo, 1951; Evans *et al.*, 2006).

The InsideWood search using these features: 13p (simple perforation plates), 22p (intervessel pits alternate), 25p (small pits), 29p (vestured pits) 30p (vessel-ray pits with distinct borders), 58p (gums and other deposits in heartwood vessels), 47p (five to 20 vessels/mm^2), 66p (non-septate fibres present), 79p (axial parenchyma vasicentric), 80p (axial parenchyma aliform), 83p (axial parenchyma confluent), 89p (axial parenchyma in marginal or in seemingly marginal bands), 97p (rays one to three cells wide), 104p (all rays cells procumbent), 115p (ten rays/mm), with no allowable mismatches, showed that the *Parapiptadenioxylon pararigida* closely resembles *Parapiptadenia rigida*, by the predominance of solitary vessels and marginal axial parenchyma (Cozzo, 1951; Tortorelli, 1956; Evans *et al.*, 2006).

The least related species were: *Caesalpinia spinosa* (Mol.) Kuntze that differs because of the predominance of rays two to three cells wide with prismatic crystals, and large intervessel pits (Detienne & Jacquet, 1983); a species of *Albizia* Durazz. by having multiseriate rays, septate fibres and prismatic crystals in chambered axial parenchyma cells (Miller, 2007); and *Copaifera langsdorffii* Desf. because of its multiseriate and heterocellular rays and axial canals in long tangential lines (Scheel-Ybert & Gonçalves, 2017). *Peltophorum dubium* (Spreng.) Taub. differs by having a predominance of rays two to three cells wide, confluent axial parenchyma and crystals in the axial parenchyma (Detienne & Jacquet, 1983; Ramos *et al.*, 2014).

Comparisons with fossil woods

The search also showed that the fossil species *Menendoxylon vasallensis* Lutz of Franco & Brea (2013) differs by having minute intervessel pits, prismatic crystals in chambered axial parenchyma cells and partially storied axial parenchyma. The InsideWood database indicates the code 120v (axial parenchyma and/or vessel elements storied) for this fossil species. However, the description in Franco & Brea (2013) indicates code 122p (rays and/or axial elements irregularly storied present).

Parapiptadenioxylon pararigida differs from *Piptadenioxylon* by having rays two to three cells wide and the absence of aliform and confluent axial parenchyma (Suguio & Mussa, 1978). *Anadenantheroxylon* Brea, Aceñolaza & Zucol differs by having large intervessel pits and multiseriate rays (Brea *et al.*, 2001; Franco & Brea, 2013). As a difference, *Microlobiusxylon* has high rays, abundant axial parenchyma and crystals in

the parenchyma (Franco & Brea, 2011). In addition, *Cylicodiscuxylon paragabunensis* Moya & Brea differs by having rays > 12 cells high, a predominance of rays that are two cells wide and prismatic crystals in the parenchyma (Moya & Brea, 2015).

Although the fossil wood studied here shares some anatomical elements with the fossil genera of Mimosoideae that have already been described, the unique set of anatomical features (> 80% uniseriate rays, axial parenchyma in marginal or in seemingly marginal bands, short and rays irregularly storied and parenchyma strands two- to ten-chambered without crystals) allow the creation of the new fossil species.

GENUS *PSEUDOPIPTADENIOXYLON* GEN. NOV. RAMOS, BREA, KRÖHLING & CONTRERAS

Type species: Pseudopiptadenioxylon uniseriatum gen. nov. & sp. nov. Ramos, Brea, Kröhling & Contreras
Pseudopiptadenioxylon uniseriatum gen. nov. & sp. nov. Ramos, Brea, Kröhling & Contreras (Fig. 3A–I).

Etymology: The generic name, *Pseudopiptadenioxylon*, refers to its affinity with the *Pseudopiptadenia*. The specific name, *uniseriatum*, refers to the presence of uniseriate rays.

Genus and species diagnosis: Growth ring boundary, demarcated by narrow marginal parenchyma bands and radially flattened and slightly thick-walled fibres. Intervessel pits medium to small. Axial parenchyma paratracheal aliform, vasicentric and confluent; axial parenchyma apotracheal marginal. Rays uniseriate. Fibres non-septate, rarely septate. Parenchyma strands of more than eight cells.

Holotype: CIDPALBO-MEG 132—CIDPALBO-MIC 1555 (three microscopic slides).

Paratype: CIDPALBO-MEG 128—CIDPALBO-MIC 1575 (three microscopic slides).

Repository: Laboratorio de Paleobotánica, CICYTTP (CONICET-Prov. ER-UADER).

Stratigraphic unit: El Palmar Formation, Late Pleistocene.

Locality: Arroyo Yuquerí, Entre Ríos province, Argentina.

Search criteria: InsideWood: 5p 13p 22p 25p 26p 29p 30p 42p 47p 52p 58p 66p 69p 79p 80p 82p 83p 89p 91p 92p 96p 104p 113a 115p 118a (IAWA features).

Description

Growth ring boundary, demarcated by axial parenchyma narrow marginal with lines up to three cells wide and by radially flattened latewood fibres (Fig. 3A). Wood diffuse-porous. Solitary vessels (77%), in radial multiples of two (15%) and three elements (8%) are circular to oval in outline, tangential diameter 91 (40–140) µm; radial diameter 103 (25–196) µm, thin walls 10 (5–14) µm thick, vessels 12 (eight to 14)/mm^2, vessel element length 198 (117–254) µm; perforation plates simple. Intervessel pits alternate, vestured, diameter 7 (5–10) µm (Fig. 3A, E, F, H, I). Vessel-ray parenchyma pits similar in shape to intervessel pits. Tyloses or/and other deposits in vessels (Fig. 3E).

Axial parenchyma paratracheal vasicentric, aliform and occasionally rare confluent; axial parenchyma apotracheal marginal (Fig. 3A, E). Parenchyma strand with more than eight cells (Fig. 3C).

Rays 12 (nine to 16)/mm, uniseriate (90%) and two cells wide (10%), 26 (18–40) µm in width; height 197 (58–394) µm or 13 (two to 23) cells (Fig. 3I, J), all ray cells procumbent (Fig. 3B, C, G).

Fibres non-septate and although seldom are septate, polygonal, angular and oval in outline; diameter 13 (10–18) µm, and thick-walled (Fig. 2D).

Affinity and comparisons

In the first search, we input mainly qualitative characters observed in both wood types (CIDPALBO-MEG 141 and 123): 5p 13p 22p 29p 30p 58p 66p 69p 79p 80p 82p 83p 89p 91p 92p 96p 104p 115p with no allowable mismatches. The results showed an affinity with four species of Fabaceae: *Microberlinia bisulcata* A.Chev., which differs mainly by having multiseriate rays and intercellular canals of traumatic origin; *Tetraberlinia bifoliolata* (Harms) Hauman, which differs by having multiseriate and heterocellular rays (Richter & Dallwitz, 2000) and *Pterocarpus dalbergioides* Roxb. ex DC., which differs by having vessels of two distinct diameter classes, axial parenchyma diffuse-in-aggregates and storied structure (Kribs, 1968). The material showed a clear affinity to *Pseudopiptadenia psilostachya* (DC.) Lewis & Lima (Detienne & Jacquet, 1983). In *Pseudopiptadenia*, *Pseudopiptadenia suaveolens* (Miq.) Grimes differs from *Pseudopiptadenioxylon uniseriatum* by having small intervessel pits (≤ 6 µm) and *Pseudopiptadenia contorta* (DC.) Lewis & Lima differs by having crystals in the fibres and a high proportion of confluent axial parenchyma; these features are not predominant in the fossil (Evans *et al.*, 2006; León, 2008).

Comparisons with fossil woods

Pseudopiptadenioxylon uniseriatum was compared with fossil genera of the *Piptadenia* group, such as

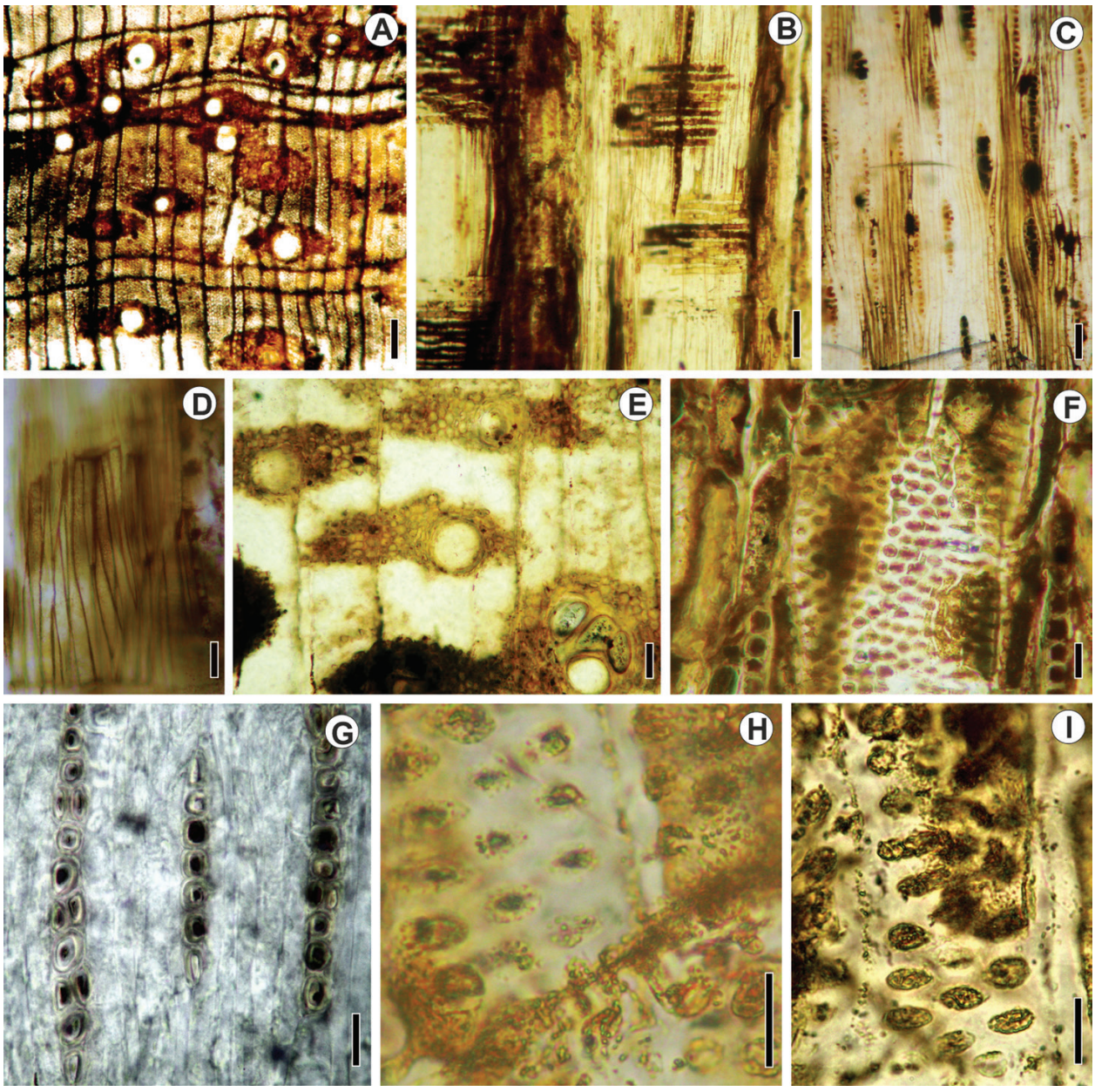

Figure 3. *Pseudopiptadenioxylon uniseriatum* gen. nov. & sp. nov. Ramos Brea Kröhling & Contreras. (Material examined CIDPALBO-MEG 128–CIDPALBO-MIC 1575: B, C, E, F, H, I; CIDPALBO-MEG 132–CIDPALBO-MIC 1555: A, D, G). A, TS general view showing vessels and fibres distribution, apotracheal and paratracheal axial parenchyma, 200 µm. B, RLS general view showing homocellular rays, 100 µm. C, TLS detail of rays uniseriate, 100 µm. D, TLS detail of fibres non-septate, 20 µm. E, TS detail of vessels and aliform and confluent axial parenchyma, 100 µm. F, RLS detail of small to medium, bordered, alternate and vestured intervessel pits, 20 µm. G, TLS detail of rays uniseriate, 20 µm. H, TLS detail of intervessel pits, 10 µm. I, TLS detail of vestured intervessel pits, 10 µm.

Microlobiusxylon that differs by having crystals in chambered axial parenchyma cells and predominance of confluent axial parenchyma. *Anadenantheroxylon* and *Piptadenioxylon* show differences in the development of confluent axial parenchyma, rays with more than one cell wide and large intervessel pits (Suguio & Mussa, 1978; Brea *et al.*, 2001). In *Menendoxylon*, *Menendoxylon vasallensis* (*sensu* Lutz, 1979) differs by having irregularly storied rays and rays three cells wide. *Cylicodiscuxylon*

paragabunensis differs by having a predominance of rays two cells wide, prismatic crystals in the parenchyma and a low density of vessels (Moya & Brea, 2015). This comprehensive review of fossil woods of the *Piptadenia* group demonstrates the uniqueness of the new species described in this article, *Pseudopiptadenioxylon uniseriatum*, and related to the extant *Pseudopiptadenia*.

GENUS *MICROLOBIUSXYLON* FRANCO & BREA

Type species *Microlobiusxylon paranaensis*

Microlobiusxylon parafoetidus sp. nov. Ramos, Brea, Kröhling & Contreras (Fig. 4A–I).

Etymology: The specific name *parafoetidus* is due to its affinity with the extant species *Microlobius foetidus* Sousa & Andrade.

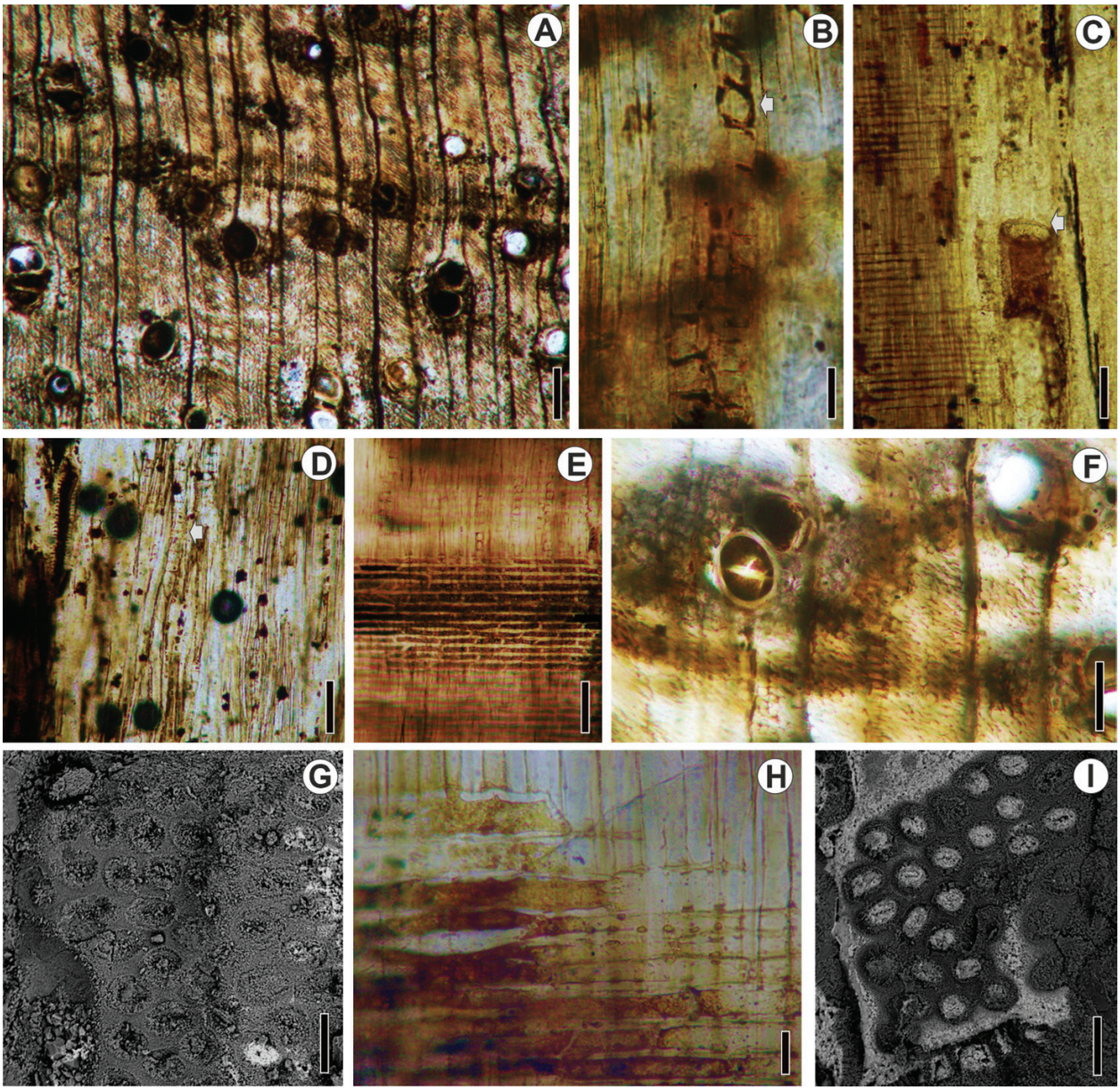

Figure 4. *Microlobiusxylon parafoetidus* sp. nov. Ramos Brea Kröhling & Contreras. (Material examined CIDPALBO-MEG 123-CIDPALBO-MIC 1546). A, TS Wood diffuse-porous. Axial parenchyma aliform and marginal, 200 µm. B, TLS crystals in chambered axial parenchyma cells, 20 µm. C, RLS simple perforation plates, 100 µm. D, TLS rays, vessel elements and cells per parenchyma strand, 100 µm. E, RLS general view showing homocellular rays and axial parenchyma, 100 µm. F, TS detail of confluent axial parenchyma, 100 µm. G, TLS detail of vestured and alternate intervessel pits (SEM), 10 µm. H, RLS detail of procumbent cells, 20 µm. I, RLS detail of vessel-ray pits with distinct borders (SEM), 10 µm.

Species diagnosis: Growth ring boundary, demarcated by narrow marginal parenchyma bands of three to five cells wide. Wood diffuse-porous. Intervessel pits small to medium. Axial parenchyma vasicentric, aliform and confluent; axial parenchyma apotracheal marginal. Rays exclusively uniseriate, occasionally rare with up to three cells wide. Crystals in chambered axial parenchyma cells.

Holotype: CIDPALBO-MEG 141—CIDPALBO-MIC 1564 (three microscopic slides).

Paratype: CIDPALBO-MEG 123—CIDPALBO-MIC 1546 (six microscopic slides).

Repository: Laboratorio de Paleobotánica, CICYTTP (CONICET-Prov. ER-UADER).

Stratigraphic unit: El Palmar Formation, Late Pleistocene.

Locality: Arroyo Yuquerí, Entre Ríos province, Argentina.

Search criteria InsideWood: 5p 13p 29p 66p 79p 80p 83p 81p 97p 104p 106p 136p 142p 25p 41p 47p 52p 92p 115p (IAWA features).

Description

Growth ring boundary, demarcated by narrow axial parenchyma marginal and occasionally development of fibres with thicker walls (Fig. 4A). Wood diffuse-porous. Vessels solitary (84%) and in radial multiples of two and three elements (16%), are circular to oval in outline, tangential diameter 86 (33–127) µm, radial diameter 85 (38–153) µm, walls 9 (5–13) µm thick, 12 (eight to 15) vessel/mm^2, vessel elements length 225 (125–260) µm, perforation plates simple, with oblique end walls (Fig. 4C, F), intervessel pits alternate, vestured and oval, diameter 9 (6–10) µm (Fig. 4G). Vessel-ray parenchyma pits small (2–5 µm diameter) (Fig. 4I). Tyloses or/and other deposits are present in vessels (Fig. 4A, F).

Axial parenchyma paratracheal aliform, vasicentric and confluent; axial parenchyma scanty apotracheal marginal (Fig. 4A, F).

Rays eight to 13/mm, uniseriate (90%), rare two to three cells wide (10%), 25 (17–31) µm in width, height 220 (71–280) µm or 16 (four to 27) cells high, all rays cells procumbent (Fig. 4C–E, H).

Fibres non-septate, and occasionally rare are septate, polygonal, angular and oval in outline, diameter 12 (7–18) µm and thick-walled (Fig. 4B, D). Crystals in chambered axial parenchyma cells, one crystal per chamber (Fig. 4B, E).

Affinity and comparisons

The following quantitative and qualitative characters observed in the fossil woods were input with zero allowed mismatches: 5p 13p 29p 66p 79p 80p 83p 81p 97p 104p 106p 136p 142p 25p 41p 47p 52p 92p 115p. The results of this search comprised five species: three Combretaceae [*Terminalia subserrata* H.Perrier, *T. seyrigii* (H.Perrier) Capuron and *T. seyrigii* var. *divaricatopsis* Capuron], which differ by having crystals in rays, axial parenchyma and fibres, and rays are heterocellular and the axial parenchyma is scarce (Detienne & Jacquet, 1983); *Pericopsis elata* (Harms) Meeuwen (Fabaceae), which differs by having stratified structure (Gasson, 1994); and *Parapiptadenia excelsa* (Griseb.) Burkart differs by having rays three cells wide (Tortorelli, 1956).

The features of fossil material place them in the *Piptadenia* group in the genus *Microlobius* (Tortorelli, 1956; Brazier, 1958; Evans *et al.*, 2006). In fact, the features (alternate and vestured intervessel pits, vasicentric, confluent and marginal axial parenchyma, uniseriate and homocellular rays, crystals in the axial parenchyma) identified by Tortorelli (1956) are shared with *Microlobiusxylon parafoetidus* or supplementary.

Comparisons with fossil woods

Table 1 expresses the differences between fossil genera with *Microlobiusxylon parafoetidus*: *Menendoxylon* and *Anadenantheroxylon* have medium to large intervessel pits and a low proportion of axial parenchyma. *Piptadenioxylon* differs by having rays two to three cells wide and only vasicentric axial parenchyma (Suguio & Mussa, 1978).

Cylicodiscuxylon paragabunensis differs by having a predominance of rays two cells wide, small intervessel pits and lack of marginal or terminal axial parenchyma (Moya & Brea, 2015).

In general, the specimens are related to *Microlobiusxylon*, although the variations in the axial parenchyma are remarkable. *Microlobiusxylon parafoetidus* has frequent confluent axial parenchyma, intervessel pits *c.* 6 µm in diameter and crystals in chambered axial parenchyma cells. These features are in *Microlobius foetidus*. *Microlobiusxylon paranaensis* has growth ring boundaries absent, but rays up to 520 µm long, high vessel density/mm^2 and minute intervessel pits, features not observed in *Microlobiusxylon parafoetidus*. Therefore, a new fossil species, *Microlobiusxylon parafoetidus*, is proposed that is closely related to the modern *Microlobius foetidus* (*sensu* Tortorelli, 1956).

GENUS *ANADENANTHEROXYLON* (BREA, ACEÑOLAZA & ZUCOL) EMEND. FRANCO & BREA (FRANCO & BREA, 2013).

Type species *Anadenantheroxylon villaurquicense* Brea, Aceñolaza & Zucol (Brea *et al.*, 2001).

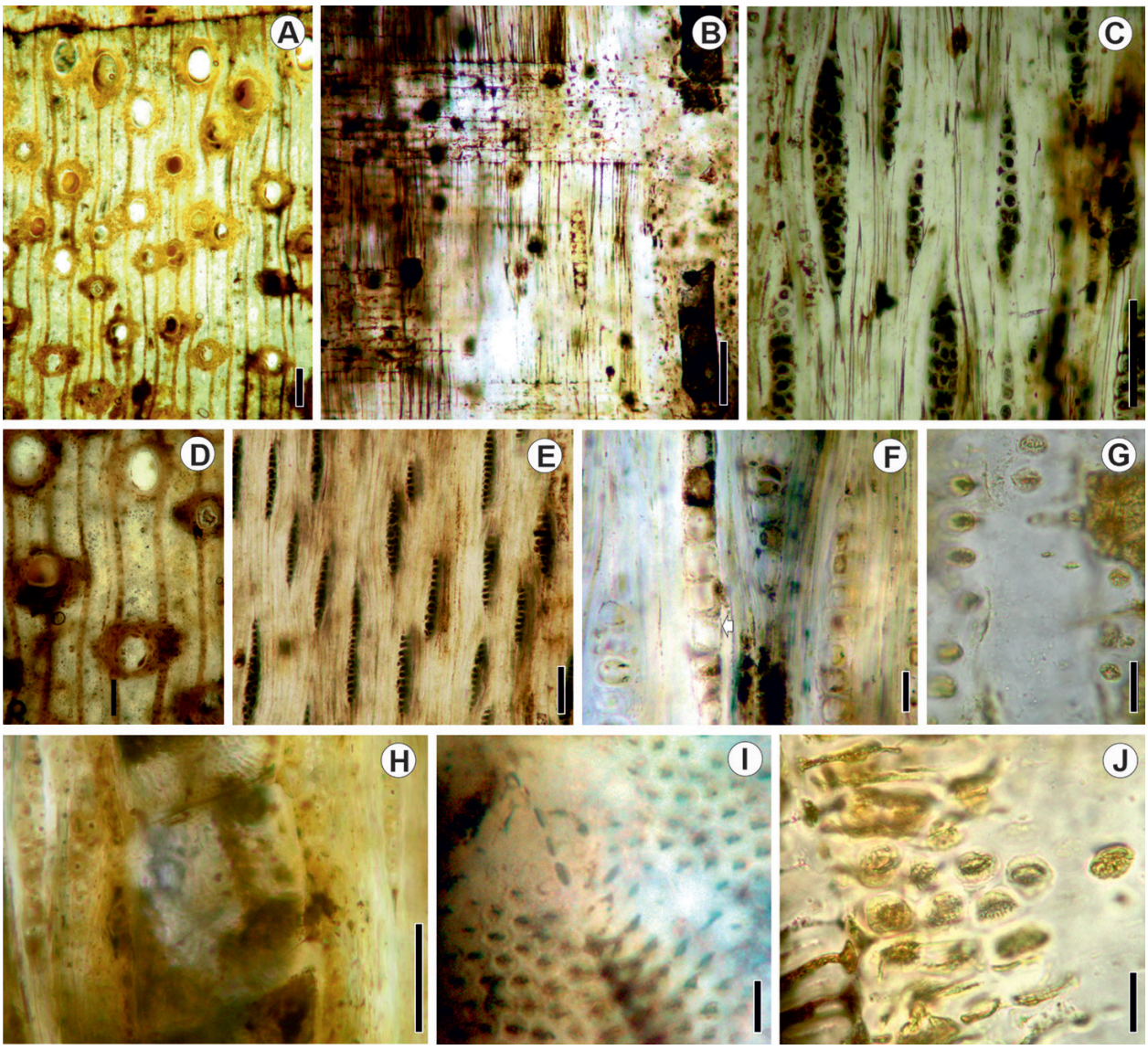

Figure 5. *Anadenantheroxylon kurupaum* sp. nov. Ramos Brea Kröhling & Contreras. (Material examined CIDPALBO-MEG 137-CIDPALBO-MIC 1560). A, TS diffuse-porous, vasicentric axial parenchyma, 200 µm. B, RLS general view showing homocellular rays composed by procumbent cells, 100 µm. C, TLS detail of rays, 100 µm. D, TS detail of vessels and aliform axial parenchyma, 100 µm. E, TLS detail of uniseriate rays, 100 µm. F, TLS detail of prismatic crystals in chambered axial parenchyma cells, 20 µm. G, RLS detail of vessel-ray pits with distinct borders, 10 µm. H, TS detail of vessel element short and rays uni-biseriate, 20 µm. I, RLS detail of medium to small, bordered, alternate, oval and vestured intervessel pits, 10 µm. J, TS detail of vestured intervessel pits, 10 µm.

Anadenantheroxylon kurupaum sp. nov. Ramos, Brea, Kröhling & Contreras (Fig. 5A–J).

Etymology: The specific name, *kurupaum*, refers to the Guarani term '*Kurupa'y*' for a hardwood tree, and it also has a more complex connotation in the culture. Some *Anadenanthera* spp. are also part of the cultural heritage and used for rituals and medicine or seen as holy trees by groups of native South American people, such as Guarani and Wichi.

Species diagnosis: Growth ring boundary, demarcated by axial parenchyma marginal narrow and by radially flattened latewood fibres. Intervessel pits small to medium. Axial parenchyma paratracheal, vasicentric, aliform (rhomboidal shape), and apotracheal diffuse

and marginal. Rays one to three cells wide. Crystals in chambered axial parenchyma cells.

Holotype: CIDPALBO-MEG 137—CIDPALBO-MIC 1560 (three microscopic slides).

Repository: Laboratorio de Paleobotánica, CICYTTP (CONICET-Prov. ER-UADER).

Stratigraphic unit: El Palmar Formation, Late Pleistocene.

Locality: Arroyo Yuquerí, Entre Ríos province, Argentina.

Search criteria InsideWood: 5p 13p 22p 29p 30p 58p 61p 70p 71p 76p 79p 80p 81p 83p 91p 92p 97p 104p 115p 136p 138a 142p (IAWA features).

Description

Growth ring boundary, demarcated by parenchyma marginal narrow and radially flattened and slightly thick-walled fibres, in some sectors (Fig. 5A). Wood diffuse-porous. Vessels solitary (66%) and in radial multiples of two (21%) and of three elements (12%), circular to oval in outline in cross-section (Fig. 5A, D), tangential diameter 108 (46–183) µm, radial diameter 121 (50–216) µm, thin walls 12 (7–15) µm thick, 11 (seven to 18)/mm². Tyloses or/and other deposits are present in vessels (Fig. 5A). Vessel elements length 256 (177–400) µm. Perforation plates simple, with horizontal to oblique end walls (Fig. 5H). Intervessel pits oval, alternate and vestured, diameter 7 (5–10) µm (Fig. 5I, J). Vessel-ray parenchyma pits similar in shape to intervessel pits, but smaller in size (Fig. 5G).

Axial parenchyma abundant paratracheal vasicentric, aliform (rhomboidal shape), confluent; axial parenchyma apotracheal diffuse and marginal (Fig. 5A, D).

Rays ten (eight to 15)/mm, two cells wide (61%), uniseriate (30%) and scanty with three cells wide (9%), 32 (20–56) µm in width, height 245 (88–381) µm or 14 (four to 24) cells high, are low and narrow; all rays cells procumbent (Fig. 5B, C, E).

Fibres, non-septate and rarely septate, are polygonal, angular and oval in outline, diameter 13 (8–20) µm and thick-walled (Fig. 5B, F).

The crystals are present in chambered axial parenchyma cells, with one crystal per chamber (Fig. 5F).

Affinity and comparisons

Adding fossil wood characteristics, such as 5p 13p 22p 29p 30p 58p 61p 70p 71p 76p 79p 80p 81p 83p 91p 92p 97p 104p 115p 136p 138a 142p in an InsideWood database search with no mismatches allowed, resulted in a group of species matching the selected characteristics: *Colophospermum mopane* (Kirk ex Benth.) J.Léonard, which differs from *Anadenantheroxylon kurupaum* by having axial parenchyma in narrow bands and vessels in radial arrangement (Gasson *et al.*, 2003); *Prosopis juliflora* (Sw.) DC., which differs by having multiseriate rays and helical thickenings in vessel elements (Evans *et al.*, 2006); and *Xylia xylocarpa* (Roxb.) Taub., which differs by having high rays and vessels arrangement in radial pattern (Pearson & Brown, 1932). *Anadenantheroxylon kurupaum* is more compatible with *Anadenanthera* and with *A. colubrina* (Vell.) Brenan, the correlation of features is expressed in diagnosis (Tortorelli, 1956; Richter & Dallwitz, 2000). *Anadenanthera colubrina* var. *cebil* (Griseb.) Altschul that inhabits the Pantanal of Mato Grosso (the world's largest wetland, Brazil), has rays one to three cells wide (rarely four cells wide) without prismatic crystals, axial parenchyma vasicentric, aliform and confluent with crystals, features perceived in *Anadenantheroxylon kurupaum* (Póvoa de Mattos, 2003; Evans *et al.*, 2006). The wood of *Anadenanthera colubrina*, studied by Guimarães (2009) in the Rio de Janeiro area (Brazil), only differs by having prismatic crystals in fibres. According to this comparison, *Anadenantheroxylon kurupaum* is most closely related to *Anadenanthera colubrina* from the Pantanal, Mato Grosso (Póvoa del Mattos, 2003).

Comparisons with fossil woods

Dalbergioxylon Ramanujam (Ramanujam, 1960) is assigned to Papilionoideae and has storied structure and banded axial parenchyma. These features are absent in *Anadenantheroxylon*. *Menendoxylon vasallensis* Lutz (Lutz, 1979) and *Piptadenioxylon* (Suguio & Mussa, 1978) differ by having partial storied structure and axial parenchyma with short bands, not observed in the *Anadenantheroxylon kurupaum*. *Albizzium* Prakash differs in the type of intervessel pits, diffuse axial parenchyma and fibres septate (Prakash, 1973).

Microlobiusxylon differs from *Anadenantheroxylon kurupaum* by having rays one or two cells wide and with small intervessel pits (Franco & Brea, 2011). The new species *Pseudopiptadenioxylon uniseriatum* differs by having a predominance of uniseriate rays and strand parenchyma with more than eight cells and the absence of crystals. *Anadenantheroxylon kurupaum* differs from *Cylicodiscuxylon paragabunensis* by having marginal axial parenchyma, scarce proportion

of parenchyma axial, and low vessels per mm^2 (Moya & Brea, 2015).

Anadenantheroxylon kurupaum sp. nov. has features that place it in the *Anadenantheroxylo*n fossil genus. However, *Anadenantheroxylon villaurquicense* differs from *Anadenantheroxylon kurupaum* and from the extant *Anadenanthera colubrina* by the absence of diffuse axial parenchyma, two to four cells per parenchyma strand and the predominance of small to medium intervessel pits (Tortorelli, 1956; Mattos *et al.*, 2003; Scheel-Ybert & Gonçalves, 2017).

TRIBE INGEAE

GENUS *CHLOROLEUCOXYLON* GEN. NOV. RAMOS, BREA, KRÖHLING & CONTRERAS

Type species: Chloroleucoxylon yukeriense gen. nov. & sp. nov. Ramos, Brea, Kröhling & Contreras.

Chloroleucoxylon yukeriense gen. nov. & sp. nov. Ramos, Brea, Kröhling & Contreras (Fig. 6A–J).

Etymology: The generic name, *Chloroleucoxylon*, refers to its affinity with the genus *Chloroleucon*

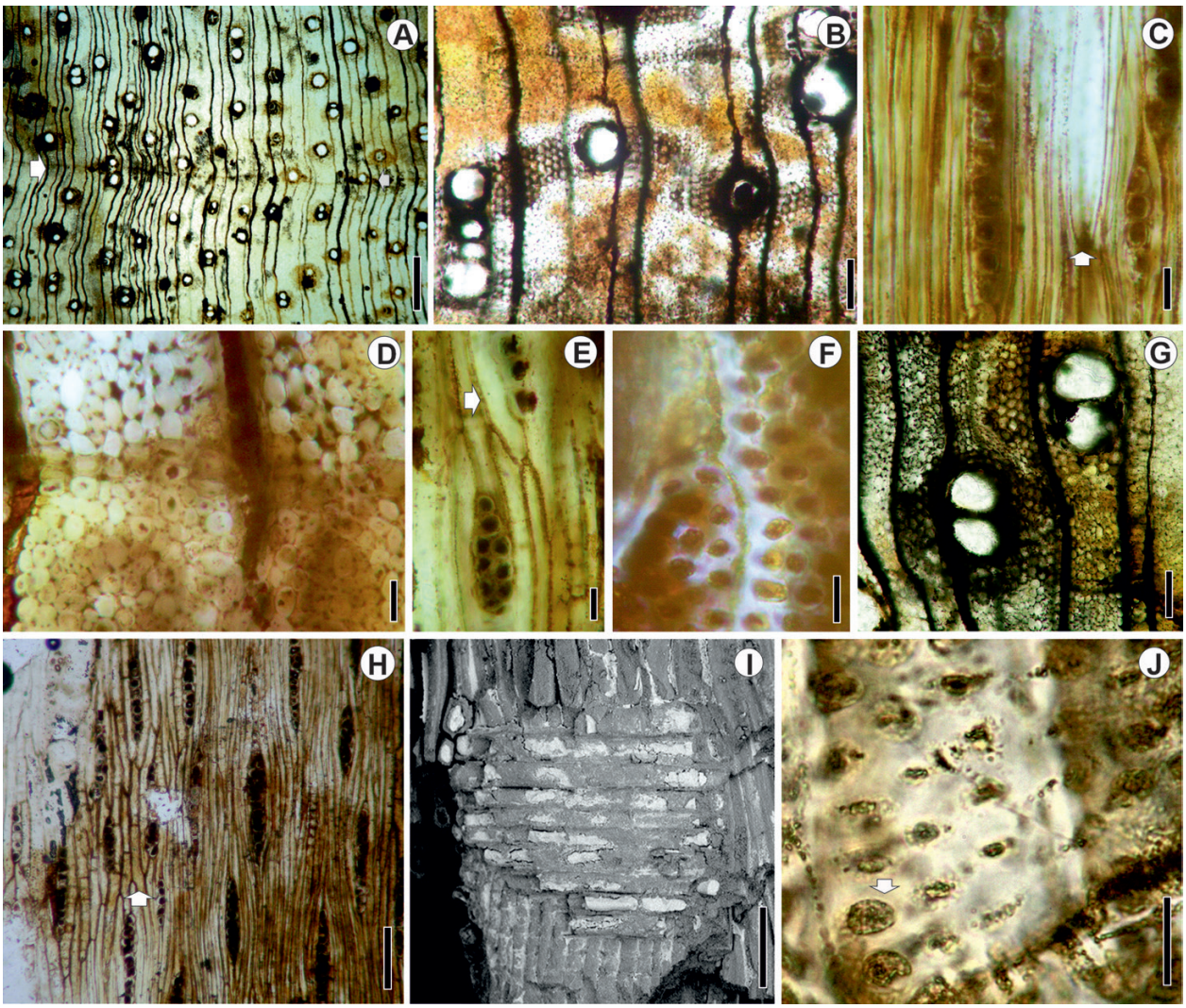

Figure 6. *Chloroleucoxylon yukeriense* gen. nov. & sp. nov. Ramos Brea Kröhling & Contreras. (Material examined CIDPALBO-MEG 117-CIDPALBO-MIC 1540). A, TS general view showing vessel distribution, axial parenchyma and growth rings (arrow), 500 µm. B, TS detail of confluent axial parenchyma, 100 µm. C, TLS detail of uniseriate rays, non-septate fibres and diffuse axial parenchyma (arrow), 20 µm. D, TS detail of marginal axial parenchyma (arrow), 20 µm. E, TLS detail ray surrounded by parenchyma strand (arrow), 20 µm. F, TLS detail of alternate and vestured intervessel pits, 10 µm. G, detail of vessels with aliform and diffuse axial parenchyma, 100 µm. H, TLS rays and parenchyma stand (arrow), 100 µm. I, RLS detail of procumbent cells (SEM), 50 µm. J, TLS detail of vestured intervessel pits (arrow), 10 µm.

(Benth.) Britton & Rose. The specific epithet, *yukeriense*, refers to the Guarani word 'yukerí' which means spiny plant.

Genus and species diagnosis: Growth ring boundary, demarcated by axial parenchyma in narrow bands or lines up to three cells wide. Intervessel pits medium-small. Axial parenchyma paratracheal vasicentric, aliform and confluent; axial parenchyma apotracheal diffuse and marginal in narrow bands. Rays one cell wide (or uniseriate). Fibres non-septate. Two cells per parenchyma strand and more than eight cells per parenchyma strand.

Holotype: CIDPALBO-MEG 117—CIDPALBO-MIC 1540 (three microscopic slides).

Repository: Laboratorio de Paleobotánica, CICYTTP (CONICET-Prov. ER-UADER).

Stratigraphic unit: El Palmar Formation, Late Pleistocene.

Locality: Arroyo Yuquerí, Entre Ríos province, Argentina.

Search criteria InsideWood: 5p 13p 22p 23p 25p 29p 30p 52p 61p 66p 69p 76p 79p 80p 81p 83p 91p 104p 136a (see codification in InsideWood, 2004-onwards).

Description

Growth ring boundary, demarcated by axial parenchyma in narrow bands or lines up to three cells wide. Wood diffuse-porous. vessels solitary (80%), in radial multiples of two elements (14%) and of three to five elements (7%), tangential diameter is 75 (36–114) µm, radial diameter 89 (38–135) µm, thin walls 8 (4–12) µm thick, 10 (7–12)/mm^2 (Fig. 6A, B). Vessel elements length 170 (115–250) µm. Perforation plates simple, with oblique end walls. Intervessel pits alternate, vestured medium and oval, diameter 8 (7–9) µm (Fig. 6F, J).

Axial parenchyma paratracheal vasicentric, aliform to confluent and confluent; axial parenchyma apotracheal diffuse and marginal in narrow bands or lines up to three cells wide (Fig. 6A, B, D, G).

Rays ten (nine to 12)/mm, one cell wide (90%), 33 (18–38) µm in width, height 190 (60–375) µm or 12 (three to 26) cells. All ray cells are procumbent (Fig. 6C, E, H, I).

Fibres non-septate, oval, circular to polygonal in outline, diameter 9 (6–13) µm and thick-walled (Fig. 6C, D). Parenchyma strands with two to eight or rarely more cells, without crystals (Fig. 6E, H).

Affinity and comparisons

An initial InsideWood search, with no mismatches allowed, was undertaken using the following general suite of features common to the specimen: 5p 13p 22p 23p 25p 29p 30p 52p 61p 66p 69p 76p 79p 80p 81p 83p 91p 104p 136a. We compared the results with the following taxa: *Terminalia avicennioides* Guill. & Perr. differs from *Chloroleucoxylon yukeriense* by having intercellular canals of traumatic origin and heterocellular rays. *Pterogyne nitens* Tul. differs by having a storied structure (Mattos *et al.*, 2003). *Chloroleucoxylon yukeriense* is related to *Chloroleucon*. In this genus, *Chloroleucon tenuiflorum* (Benth.) Barneby & Grimes differs by having a predominance of rays two to three cells wide (Tortorelli, 1956). However, *Chloroleucoxylon yukeriense* is closely related to *Chloroleucon mangense* Britton & Rose by having uniseriate rays, non-septate fibres and the same type of intervessel pits, and it only differs by having crystals (Cassens & Miller, 1981; Evans *et al.*, 2006).

Comparisons with fossil woods

Chloroleucoxylon yukeriense was compared with the more related fossil taxa. They integrate entities of Mimosae and Ingae: *Menendoxylon* differs by having species with rays up three cells wide and low, which does not exceed 300 µm in height. A species in the genus has a partial storied structure in the rays; this does not occur in *Chloroleucoxylon yukeriense*.

Crystals and strand parenchyma with more than eight cells are well represented in *Microlobiusxylon parafoetidus* but absent in *Chloroleucoxylon yukeriense* and *Anadenantheroxylon kurupaum*. *Zygiaxylon amazonicum* Kloster, Gnaedinger &Adami-Rodrigues has crystals and rays more than one cell wide (Kloster *et al.*, 2015), features not present in *Chloroleucoxylon yukeriense*.

Chloroleucoxylon yukeriense has marginal and diffuse axial parenchyma and short (≤ 350 µm) vessels. These features are not observed in *Abaremaxylon hydrochorea* Moya & Brea (Moya & Brea, 2015) or *Pseudopiptadenioxylon uniseriatum*. *Ingoxylon sahnii* Müller-Stoll & Mädel mainly differs by having banded axial parenchyma and multiseriate rays (Müller-Stoll & Mädel, 1967). *Paraalbizioxylon caccavariae* Martinez differs by having rays more than one cell wide and scanty axial parenchyma (Martinez, 2014). *Paraalbizioxylon yunnanensis* differs mainly by having banded axial parenchyma and rays with more than one cell wide (Cheng *et al.*, 2018).

After detailed comparison with fossil and modern species, we found this morphotype resembles the extant species *Chloroleucon mangense*. The discussion

we present here justifies the erection of a new fossil genus and species, *Chloroleucoxylon yukeriense*.

Genus *Enterolobiumoxylon* Pérez-Lara, Estrada-Ruiz & Castañeda-Posadas

Type species *Enterolobiumoxylon vassalloae* sp. nov. Ramos, Brea, Kröhling & Contreras.

Enterolobiumoxylon vassalloae sp. nov. Ramos, Brea, Kröhling et Contreras (Fig. 7A–K).

Etymology: The specific epithet, *vassalloae*, after Cristina Vassallo de Cettour in recognition of her significant and extensive work on fossils collection.

Species diagnosis: Growth ring boundary, demarcated by narrow marginal parenchyma bands and radially flattened and slightly thick-walled fibres. Intervessel pits medium-large. Axial parenchyma vasicentric paratracheal, aliform to confluent; axial parenchyma apotracheal diffuse and marginal. Rays one to three cells wide, all ray cells procumbent. Fibres non-septate. Parenchyma strand of five or more cells.

Holotype: CIDPALBO-MEG 110, CIDPALBO-MIC 1367 (three microscopic slides).

Repository: Laboratorio de Paleobotánica, CICYTTP (CONICET-Prov. ER-UADER).

Stratigraphic unit: El Palmar Formation, Late Pleistocene.

Locality: Arroyo Yuquerí, Entre Ríos province, Argentina.

Search criteria InsideWood: 5p 13p 22p 29p 30p 53p 61p 65p 66p 69p 76p 79p 80p 81p 92p 93p 97p 104p 131a (IAWA features).

Description

Growth ring boundary, demarcated by narrow marginal parenchyma bands and radially flattened and slightly thick-walled fibres (Fig. 7A). Wood diffuse-porous. Solitary vessels (73%), in radial multiples of two (21%) and three cells (6%) circular to oval in outline tangential diameter 133 (75–178) µm, radial diameter 146 (38–275) µm, thin walls 12 (8–15) µm thick 7 (4–10)/mm². Tyloses or/and other deposits in vessels (Fig. 7A, D). Vessel element length 312 (125–550) µm, are short. Perforation plates simple, with horizontal to oblique and appendix visible end walls. Intervessel pits alternate, vestured and oval, diameter 10 (7–12) µm (Fig. 7C, E, F, I–K). Vessel-ray parenchyma pits similar to intervessel pits (Fig. 7G).

Axial parenchyma paratracheal vasicentric and aliform, rare confluent; axial parenchyma apotracheal diffuse and marginal (Fig. 7A, D, E).

Rays 12 (seven to 17)/mm, two cells wide (70%), one cell wide (20%) and three cells wide (10%), 35 (15–64) µm in width, 203 (50–750) µm in height or 15 (two to 38) cells high that are low and narrow; homocellular rays formed by procumbent cells (Fig. 7B, E, G, H).

Fibres non-septate and septate, irregularly arranged, oval, circular to polygonal outline, diameter 15 (6–23) µm thick and thin-walled, diameter 4 (2–5) µm thick. Parenchyma strand of five or more cells (Fig. 7E).

Affinity and comparisons

A subsequent InsideWood search using this set of features was conducted: 5p 13p 22p 29p 30p 53p 61p 65p 66p 69p 76p 79p 80p 81p 92p 93p 97p 104p 131a. This search retrieved two species related to *Samanea leptophylla* (Harms) Brenan & Brummitt, and *Xylia xylocarpa* (Roxb.) Taub. (Ingeae), but these were eliminated, due to the following differences: the former has minute intervessel pits and predominance of confluent axial parenchyma (Louppe, Oteng-Amoako and Brink, 2008), and *Xylia xylocarpa* has crystals in cells per parenchyma strand and abundant axial parenchyma confluent (Pearson & Brown, 1932). The anatomy of *Enterolobium schomburgkii* Benth., as described in Evans *et al.* (2006) and León (2008), matches *Enterolobiumoxylonn vassalloae* sp. nov. because it has diffuse axial parenchyma, which is not present in *Enterolobium contortisiliquum* described by Tortorelli (1956). Hence, the only feature that differentiates *Enterolobiumoxylon vassalloae* from *E. contortisiliquum* (Vell.) Morong is the absence of diffuse axial parenchyma (Cozzo, 1951; Metcalfe & Chalk, 1950; Tortorelli, 1956; Tomazello Filho *et al.*, 1983; Evans *et al.*, 2006; Lima *et al.*, 2009).

Comparisons with fossil woods

Albizinium Prakash differs by having larger rays commonly four to ten cells wide and axial parenchyma with prismatic crystals (Prakash, 1973; Guleria, 1984). *Albizia* differs by having heterocellular and multiseriate rays (Prakash & Barghoorn, 1961).

Ingoxylon Mueller-Stoll and Maedel differs by having minute intervessel pits, banded axial parenchyma and multiseriate rays (Müller-Stoll & Mädel, 1967), *Paraalbizioxylon caccavariae* differs by having vessels in diagonal and/or radial pattern, prismatic crystals and lacking confluent axial parenchyma (Martinez, 2014). *Zygiaxylon amazonicum* mainly differs by having uniseriate rays, crystals and minute intervessel pits (Kloster *et al.*, 2015).

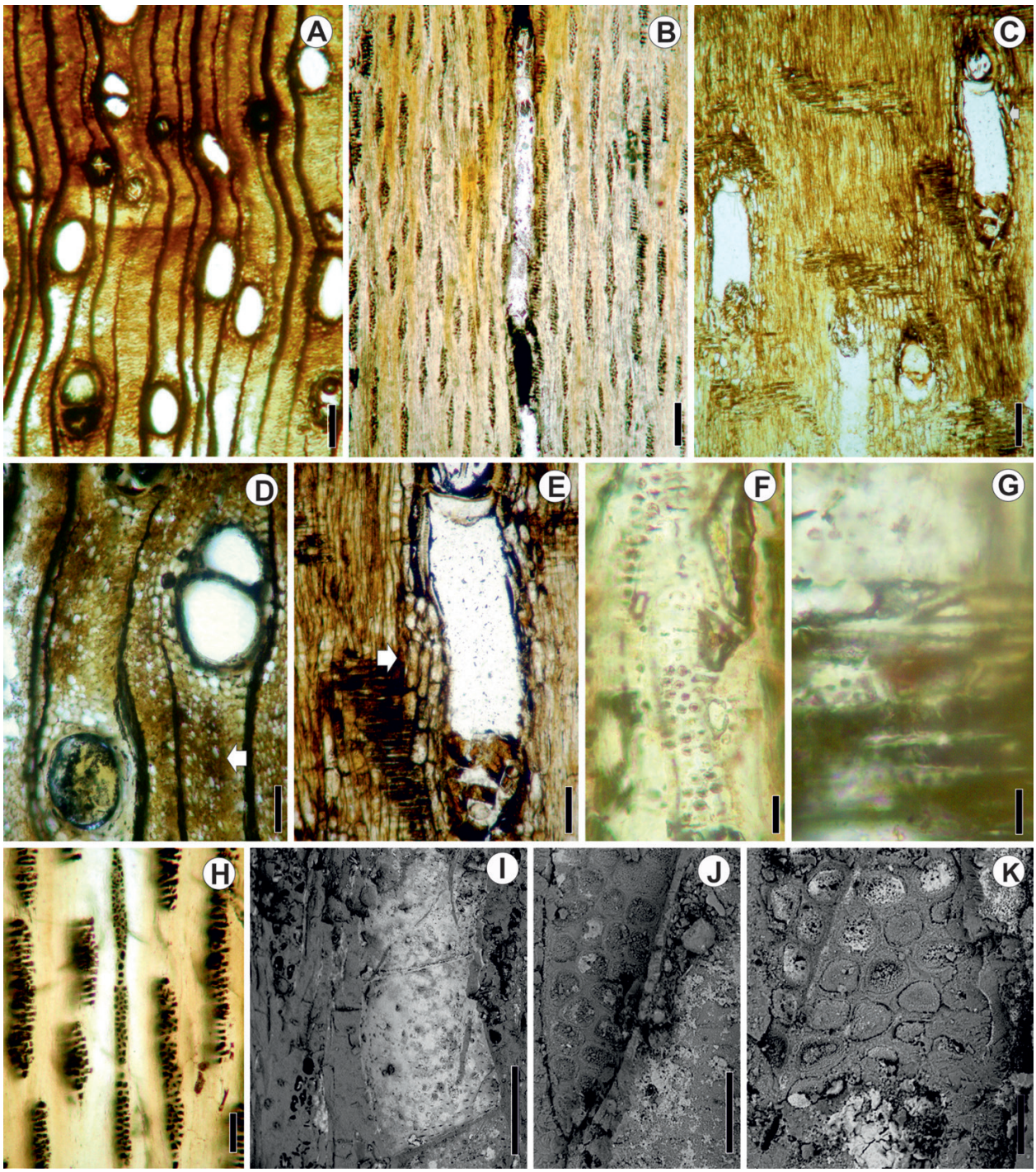

Figure 7. *Enterolobiumoxylon vassalloae* sp. nov. Ramos Brea Kröhling & Contreras. (Material examined CIDPALBO-MEG 110-CIDPALBO-MIC 1367). A, TS general view of marginal axial parenchyma and growth rings, 200 µm. B, TLS general view of ray width one to three cells, 200 µm. C, RLS general view homocellular rays and vessel elements, 200 µm. D, TS vessels in radial multiples of two and solitary, vasicentric and diffuse axial parenchyma (arrow), 100 µm. E, TLS detail of vasicentric axial parenchyma (arrow), 100 µm. F, TLS element vessel and intervessel pits, 20 µm. G, RLS vessel-ray pits with distinct borders; similar to intervessel pits in size and shape throughout the ray cell, 20 µm. H, TLS detail of rays, 100 µm. I, TLS detail of vessel element short (SEM), 80 µm. J, TLS detail of vestured intervessel pits (SEM), 20 µm. K, TLS detail of alternate and vestured intervessel pits (SEM), 10 µm.

Pons & De Franceschi (2007) describe a fossil cf. Ingeae from sediments of the Pebas Formation in Peru (Miocene). For the same geological epoch Martinez (2014) describes 'cf. Ingeae' in the Chiquimil Formation (Catamarca province, Argentina). Both differ mainly by having prismatic crystals and storied structure and the absence of diffuse axial parenchyma. *Abaremaxylon hydrochorea* has uniseriate and short rays, small to minute intervessel pits, and crystals in axial parenchyma (Moya & Brea, 2015), features that are not present in *Enterolobiumoxylon vassalloae*.

Chloroleucoxylon yukeriense differs by having small to medium intervessel pits, and a low proportion of diffuse axial parenchyma. In *Pseudopiptadenioxylon* and *Microlobiusxylon* uniseriate rays dominate; this does not occur in *Enterolobiumoxylon vassalloae*. Recently, a fossil related to *Enterolobium* was described. It is *Enterolobiumoxylon triserial* Pérez, Hernández, Romero-Saltos, Valencia from the Lower Eocene (El Bosque Formation, Chiapas, Mexico); there are some characters such as crystalliferous septate parenchyma, growth ring boundaries not found and marginal axial parenchyma not present (Pérez-Lara *et al.*, 2021), which differ from *Enterolobiumoxylon vassalloae*. Therefore, we conclude that the combination of anatomical features establishes a close relationship with the modern *Enterolobium* and propose the creation of a new fossil entity: *Enterolobiumoxylon vassalloae*.

Genus *Cedrelinga* Ducke

Type species *Cedrelinga catenaeformis* Ducke

Cedrelinga paleocatenaeformis sp. nov. Ramos, Brea, Kröhling & Contreras (Fig. 8A–L).

Etymology: Specific epithet, *palaeocatenaeformis* refers to its affinity with *Cedrelinga catenaeformis*.

Species diagnosis: Growth ring boundary, demarcated by narrow marginal parenchyma bands and by solitary vessel arrangements. Wood diffuse-porous. Solitary large vessels and radial multiples. Intervessel pits medium to large. Axial parenchyma paratracheal vasicentric to aliform and scarce confluent; axial parenchyma apotracheal. Rays uniseriate, homocellular, composed exclusively of procumbent cells. Fibres non-septate. Parenchyma strands of two to eight cells.

Holotype: CIDPALBO-MEG 127—CIDPALBO-MIC 1550.

Paratype: CIDPALBO-MEG 139—CIDPALBO-MIC 1562 (ten microscopic slides).

Repository: Laboratorio de Paleobotánica, CICYTTP (CONICET-Prov. ER-UADER).

Stratigraphic unit: El Palmar Formation, Late Pleistocene.

Locality: Arroyo Yuquerí, Entre Ríos province, Argentina.

Search criteria InsideWood: 13p 26p 29p 30p 66p 76p 79p 80p 83p 93p 96p 97p 104p 115p 136a (see codification in InsideWood, 2004-onwards).

Description

Growth ring boundary, demarcated by narrow marginal parenchyma bands and by an arrangement of vessels solitary. Wood diffuse-porous. Vessels solitary (72%), in series multiples of two elements (16%), of 3 to 7 elements (15%), tangential diameter 133 (45–216) µm, radial diameter 144 (38–254) µm, thin walls 14 (8–21) thick, 8 (4–12)/mm², oval to-circular in outline (Fig. 8A, E). Tyloses or/and other deposits in vessels (Fig. 8A, E). Vessel element length 260 (127–400) µm. Perforation plates simple, with horizontal end walls (Fig. 8C). Intervessel pits alternate, vestured and oval, mean diameter 9 (7–11) µm, are medium to large (Fig. 8J–L). Vessel-ray parenchyma pit similar in shape and size to intervessel pits (Fig. 8I).

Axial parenchyma paratracheal vasicentric to aliform, confluent; axial parenchyma apotraqueal marginal and rare diffuse (Fig. 8E).

Rays ten (seven to 12)/mm, one cell wide (92%) and uniseriate with partially two cells wide (8%), width 31 (15–50) µm, height 318 (45–699) µm or 15 (two to 40) cells high. All cells procumbent (Fig. 8B–D, H, I). Fibres non-septate, polygonal, angular and oval in outline, diameter 18 (10–30) µm (Fig. 8D, F, H). Strand parenchyma of two to eight cells (Fig. 8G).

Affinity and comparisons

InsideWood database was searched to obtain a list of extant species with the following combination of features that occur in the fossil wood: 13p 26p 29p 30p 66p 76p 79p 80p 83p 93p 96p 97p 104p 115p 136a with no allowable mismatches. According to the results of this search, the fossil woods were related to *Cedrelinga catenaeformis*.

Muñiz *et al.* (2012) described the anatomy of *Cedrelinga* from northern Mato Grosso (Brazil), with small intervessel pits and scarce axial parenchyma, whereas León (2008) in southern Venezuela observed that *C. caterniformis* has medium to large intervessel pits (11 µm) and aliform, vasicentric and diffuse axial parenchyma. Valderrama Freyre (1998) compared the branch and stem anatomy of the xylem of *Cedrelinga*

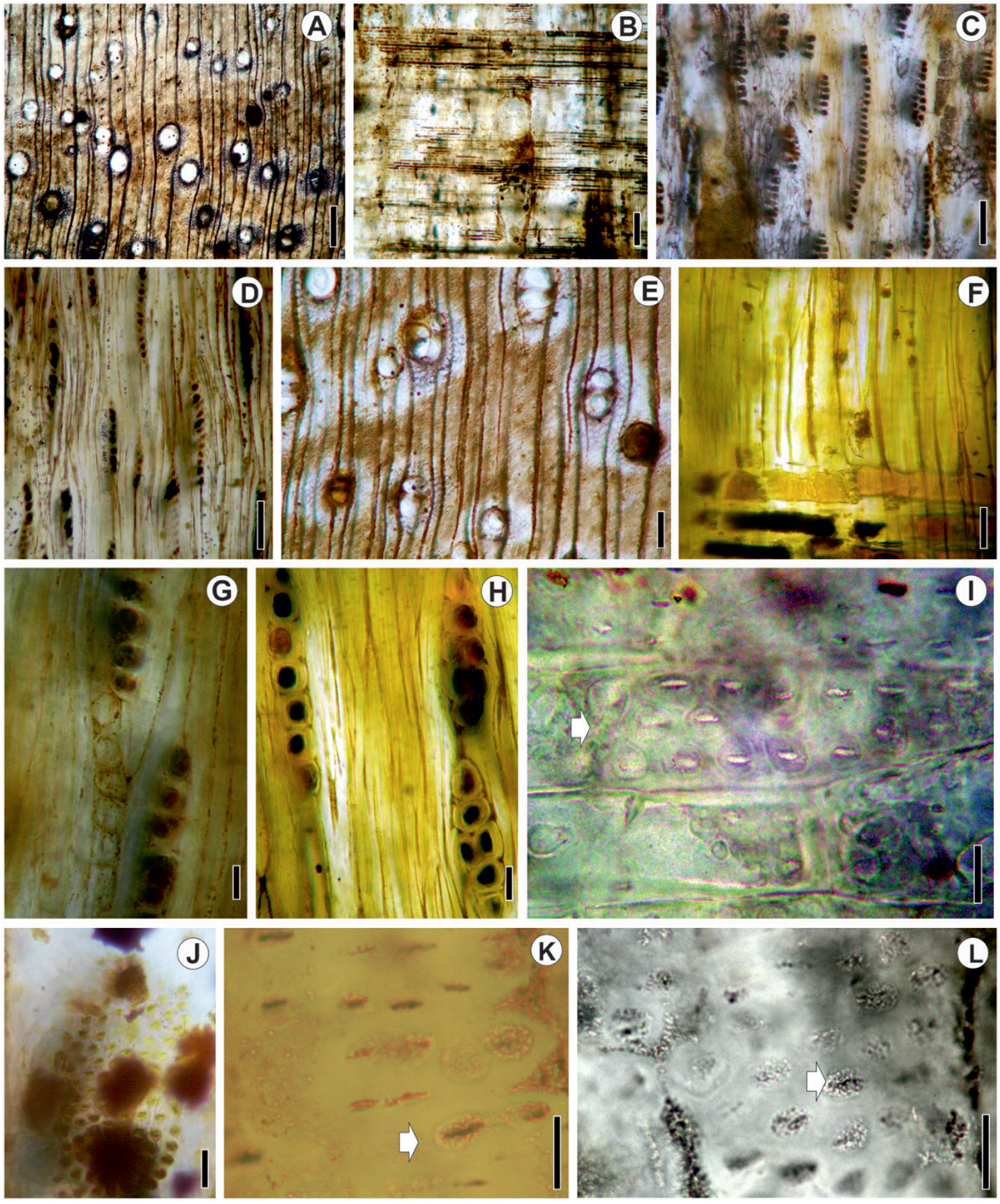

Figure 8. *Cedrelinga paleocatenaeformis* sp. nov. Ramos Brea Kröhling & Contreras. (Material examined CIDPALBO-MEG 127-CIDPALBO-MIC 1550: A, C, D, E, G, I, K, L; CIDPALBO-MEG 139-CIDPALBO-MIC 1562: B, F, H, J). A, TS general view showing vessel distribution, axial parenchyma, 400 µm. B, RLS general view of homocellular rays, 200 µm. C, TLS detail of uniseriate rays, 100 µm. D, TLS parenchyma strand without crystals (arrow) and uniseriate rays, 100 µm. E, TS vessels solitary and aliform axial parenchyma, 200 µm. F, RLS procumbent cells and non-septate fibres, 20 µm. G, TLS detail of parenchyma strand and rays, 20 µm. H, TLS detail of uniseriate rays, 20 µm. I, RLS vessel-ray pits with distinct borders; similar to intervessel pits in size and shape throughout the ray cell, 10 µm. J, TLS detail of alternate and vestured intervessel pits, 20 µm. K, TLS detail of vestured intervessel pits (arrow), 10 µm. L, TLS detail of vestured and alternate intervessel pits (arrow), 10 µm.

in samples from tropical humid forest in the Peruvian Amazon. Some features of the trunk were adjusted to the wood fossil under study, e.g. small to medium intervessel pits, uniseriate rays, non-septate fibres and type of axial parenchyma and the absence of crystals. Evans *et al.* (2006) observed septate fibres in their species, that are absent in the fossil wood studied here. In conclusion, *Cedrelinga paleocatenaeformis* has more similarities with the species described by Valderrama Freyre (1998) and León (2008).

Comparisons with fossil woods

The material was compared with fossil taxa relating to modern species of Ingeae and Mimoseae. *Enterolobiumoxylon vassalloae* differs because of the dominance of diffuse axial parenchyma and rays one to three cells wide. *Anadenantheroxylon* differs by having large intervessel pits, abundant axial parenchyma and fibres (Brea *et al.*, 2001; Franco & Brea, 2013). *Ingoxylon* differs by having banded axial parenchyma and multiseriate rays (Müller-Stoll & Mädel, 1967). *Ingoxylon bavaricum* Selmeier differs by having minute intervessel pits, tracheids and septate fibres (Selmeier, 1973). *Ingoxylon nathorstii* (Schuster) Müller-Stoll & Mädel [=*Paraalbizioxylon nathorstii* (Schuster) Gros.] differs by having septate axial parenchyma and lack of diffuse and confluent axial parenchyma (Schuster, 1910). cf. Ingeae differs by having septate fibres and small intervessel pits (Pons & De Franceschi, 2007). The fossil of the Chiquimil Formation cf. Ingeae mainly differs by having prismatic crystals in axial parenchyma and storied structure (Martinez, 2014). *Abaremaxylon hydrochorea* differs by having low rays ≤ 13 cells wide, unilateral axial parenchyma and crystals (Moya & Brea, 2015).

It has been recently found that the fossil species *Paraalbizioxylon yunnanensis* Cheng, Wang, Liu, Jin, Mehrotra, Jiang & Li of the Pliocene fluvial-lacustrine sediments from China differs by having a predominance of uniseriate and low rays and small to minute intervessel pits (Cheng *et al.*, 2018). The fossil woods from the El Palmar Formation differ from previously described fossil species. Hence, they are assigned to the new species *Cedrelinga paleocatenaeformis*, which has a close affinity with the modern *Cedrelinga catenaeformis*.

THE NEAREST LIVING RELATIVE AND COEXISTENCE APPROACH METHODS

The CA suggests that during some climatic events of the Late Pleistocene related to the development of the palaeoflora of the Arroyo Yuquerí fossiliferous locality, the MAT estimated for the Uruguay fluvial belt was *c.* 22–28°C (Table 2, Fig. 9). This range of temperatures

Table 2. Taxa used in the coexistence approach method

	Genus relative	NLR	Habitat preference	Phenology	MAT °C	MiT °C	MaT °C	MAP mm/y	MiP mm/y	MaP mm/y
1	*Chloroleucon*	*C. mangense*	HF, STr	E	25	7	35	956	569	1300
2	*Ocotea*	*O. acutifolia*	HF, STr	E	20	10	28	1370	620	2034
3	*Gossweilerodendron*	*Gossweilerodendron* sp.	HF	D	25	17	40	1825	1300	2257
4	*Parapiptadenia*	*P. rigida*	HF, STr	E-D	21	10	34	1055	330	1701
5	*Microlobius*	*Microlobius foetidus.*	HF, STr	E	24	10	34	1151	569	1465
6	*Bastardiopsis*	*B. densiflora*	HF, Str	E	21	10	34	1500	1300	1700
7	*Cedrelinga*	*C. catenaeformis*	HF, STr-DF	E	28	21	32	1800	1300	2900
8	*Pseudopiptadenia*	*P. contorta*	HF, STr	E	21	12	33	1350	1000	1600
9	*Enterolobium*	*Enterolobium* sp.	HF, STr	E-D	22	10	35	1075	569	1700
10	*Loxopterygium*	*Loxoterygium*sp.*	HF, STr	E	23	7	33	1079	567	2103
11	*Anadenanthera*	*Anadenanthera* sp.	HF, STr	*E-D	22	10	34	1250	568	1700
12	*Butia*	*Butia yatay*	S, HF	E	21	10	34	1075	569	1750

Key to abbreviations used:
Habitat preference: DF = dry forests, HF = humid forests, S = savanna with palm forests, Str = Seasonally Tropical Forests
Phenology: E = evergreen, D = deciduous

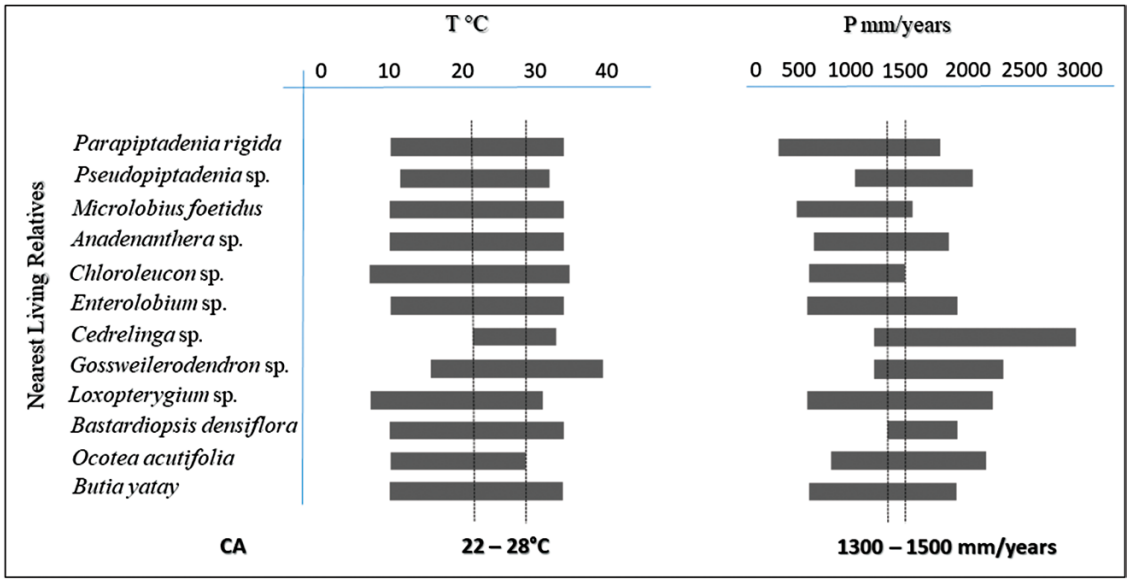

Figure 9. Palaeoclimatic values estimated by using the coexistence approach method with data derived from NLRs.

is consistent with that of woodland formations at lower latitudes (*c.* 28° and 25° S latitude) such as the Paranaense biogeographic province (Arana *et al.*, 2021). CA showed an estimated MAP between 1300 and 1500 mm/year, (Table 2, Fig. 9), indicating that during some phases of the Late Pleistocene the forests developed in the upper/middle Uruguay River Basin under humid conditions.

Vulnerability and mesomorphy indices

The VI for fossil woods ranges from seven to 19, while MI is between 592 and 1270 (Table 1). These relatively high values suggest that some phases of the Late Pleistocene were characterized by environments with high water availability and that Caesalpinioideae woods can be interpreted as mesophytes or hydrophytes in terms of xylem structure. The results the VI and MI indices indicate these plants had an efficient water conduction system.

Procrustes analysis

GPA results showed a significant consensus (75%) between the ordinations based on qualitative and quantitative features measured on fossil woods. Principal component 1 (PC 1, 58.5%) and 2 (PC 2, 41.5%) accounted for 100% of the total variation.

Overall, taking into account PC 1 with 58.5% of the explained variability, both fossils and NLRs from the same tribe were associated (Fig. 10). The taxa assigned to Ingeae, fossil and modern, grouped each other on the positive axis, or near it, whereas the fossil and modern Mimosae were grouped on the negative axis. There were exceptions, such as *Chloroleucoxylon yukeriense* (white cross 3) and *Chloroleucon mangense* (white diamond 1), which were grouped with Mimoseae. *Chloroleucon tenuiflorum* (white diamond 2) remained associated with all species of Ingeae (fossil and modern).

Another exception was the association of *Pseudopiptadenia psilostachya* (black triangle 3) and *Anadenanthera peregrina* Speg (black diamond 2) with species of Ingeae on the positive axis in PC 1 (see Fig. 10). We performed further analysis to detect the features that favoured these groupings. The axial parenchyma and vessel deposits features showed to have a strong influence on the association of *Chloroleucoxylon yukeriense* and *Chloroleucon mangense* with fossils related to Mimoseae. Despite the differences detected in quantitative features, qualitative features determined this behaviour in the cluster analysis. In addition, *Parapiptadenioxylon pararigida* (black cross 6) has irregularly storied rays and *C. mangense* has irregularly storied vessel elements and axial parenchyma, uncommon features of the group. *Parapiptadenioxylon pararigida* and *C. mangense* were probably associated because of the latter features.

As for *Anadenanthera peregrina* and *Pseudopiptadenia psilostachya*, qualitative features (marginal and diffuse axial parenchyma and ray type) strongly influenced their behaviour in the cluster analysis (CP 1). The modern species of *Parapiptadenia* and its fossil were strongly associated.

The CP 2, with 41.5% of the explained variability, segregates the fossil taxa, all the *Parapiptadenia* spp., *Cedrelinga* spp., *Anadenanthera* spp. and *Chloroleucon*

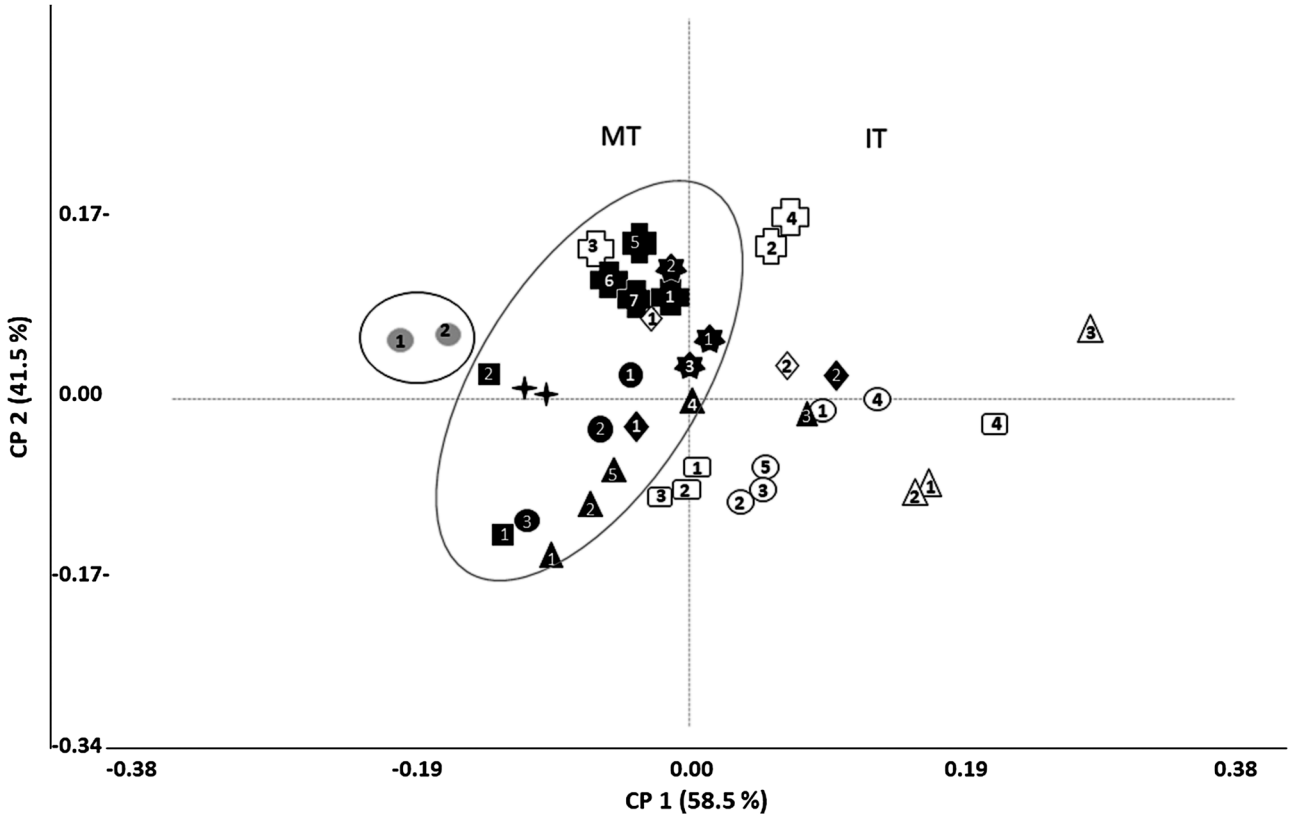

Figure 10. Procrustes comparison of the qualitative and quantitative features of the fossils and extant species. Fossil species (crosses): *Anadenantheroxylon kurupaum* (black cross 1), *Cedrelinga paleocatenaeformis* (white cross 2), *Chloroleucoxylon yukeriense* (white cross 3), *Enterolobiumoxylon vassalloae* (white cross 4), *Microlobiusxylon parafoetidus* (black cross 5), *Parapiptadenioxylon pararigida* (black cross 6) and *Pseudopiptadenioxylon uniseriatum* (black cross 7). Modern species: *Albizia inundata* (white cube 3), *Anadenanthera colubrina* (black diamond 1), *Anadenanthera peregrina* (black diamond 2), *Cadia purpurea* (grey circle 1) *Cedrelinga catenaeformis*-1 (white triangle 1), *Cedrelinga catenaeformis*-2 (white triangle 2), *Cedrelinga catenaeformis*-3 (white triangle 3), *Chloroleucon mangense* (diamond 1), *Chloroleucon tenuiflorum* (diamond 2), *Enterolobium contortisiliquum*-1 (circle 1), *Enterolobium contortisiliquum*-2 (circle 2), *Enterolobium contortisiliquum*-3 (circle 3), *Enterolobium cyclocarpum* (circle 4), *Enterolobium schomburgkii* (circle 5), *Geoffroea decorticans* (grey circle 2), *Inga alba* (white cube 4), *Microlobius foetidus* (four pointed star), *Microlobius foetidus paraguensis* (four pointed star), *Mimosa polyantha* (black cube 1), *Parapiptadenia excelsa* (black soul 1), *Parapiptadenia rigida*-1 (black soul 2), *Parapiptadenia rigida*-2 (black soul 3), *Pithecellobium saman* (synonym: *Samanae saman*) (white cube 2); *Prosopis alpaca* (black circle 1), *Prosopis kuntzei* (black circle 2); *Prosopis vinalillo* (black circle 3); *Pseudopiptadenia contorta*-1 (purple triangle 1), *Pseudopiptadenia contorta*-2 (black triangle 2), *Pseudopiptadenia psilostachya* (black triangle 3), *Pseudopiptadenia suaveolens*-1 (black triangle 4), *Pseudopiptadenia suaveolens*-2 (black triangle 5), *Vachellia caven* (black cube 2) and *Zygia longifolia* (white cube 1).

spp. on the positive axis, and most of the modern species on the negative axis. As it can be observed (Fig. 10, Appendix) this behaviour of the species responds to their quantitative features mainly vessel per mm^2, and qualitative features such as type of rays and particularities of the axial parenchyma.

In the incorporation of nine modern species of the two tribes from seasonal and tropical environments (*Inga alba* – white cube 4–, *Mimosa polyantha* – black cube 1–, *Pithecellobium saman* (Syn *Samanea saman*) – white cube 2–, *Prosopis alpaca* – black circle 1–, *Prosopis kuntzei* – black circle 2–, *Prosopis vinalillo* – black circle 3–, *Vachellia caven* – black cube 2– and *Zygia longifolia* – white cube 1–), these were grouped closely with their corresponding tribes, on the negative axis of CP 2 and away from the fossils (Fig. 10). This distribution is explained by quantitative features such as vessels per mm^2 and quantitative features such as ray width, ray type and axial parenchyma. The outgroup taxa (*Cadia purpurea* – grey circle 1– and *Geoffroea decorticans* – grey circle 2–) did not group with the other ones, the determining features being vessel parameters, ray height and banded axial parenchyma.

DISCUSSION

PALAEOBOTANICAL AND BIOGEOGRAPHIC SIGNIFICANCE

Fabaceae are distributed worldwide, but Caesalpinioideae are mainly tropical and subtropical woody trees, shrubs or lianas with diverse species in Southeast Asia, Africa and South America (Klitgård & Lewis, 2010; LPWG, 2017). A small diversity of fossil species with anatomical features of Caesalpinioideae from southern South America in the Late Pleistocene has been recorded (Pujana *et al.*, 2011; Ramos *et al.*, 2014). The variability in fossil wood anatomy reflects the wide diversity of Fabaceae in the Pleistocene in the study area (Brea *et al.*, 2010; Ramos *et al.*, 2012, 2014, 2017; Ramos, 2015). The increase in the records of fossil genera in the subfamily and tribes reduces the knowledge gap between modern and old diversity of Fabaceae, and the detail and thoroughness in the analysis and comparisons of qualitative and quantitative features support a close approximation to the genera assigned in this work. Indeed, the creation of fossil genera and fossil species derived from their NRL is consistent.

Subfamilies of Fabaceae can be differentiated by wood anatomy (Cozzo, 1951; Metcalfe & Chalk, 1950; Baretta-Kuipers, 1981). In this work, a partial tribe differentiation can be observed in Caesalpinioideae (Fig. 10, Appendix).

The present study adds seven taxa of angiosperms for the Late Pleistocene of north-eastern Argentina, based on 11 fossil woods. The analysis of more fossil woods found in fluvial units of the middle Uruguay Basin is in progress, but preliminary results indicate that there are several angiosperm taxa with wood anatomy resembling that of Mimoseae and Ingeae (Table 2 and Appendix). They include the fossil genera *Parapiptadenioxylon* gen. nov., *Pseudopiptadenioxylon* nov. gen., *Microlobioxylon parafoetidus* sp. nov., *Anadenantheroxylon*, *Enterolobiumoxylon vassalloae*, *Chloroleucoxylon* gen. nov. *Cedrelinga paleocatenaeformis* sp. nov. and the modern species, *Parapiptadenia rigida, Microlobius foetidus*, *Pseudopiptadenia* sp., *Anadenanthera colubrina*, *Enterolobium* sp., *Chloroleucon mangense* and *Cedrelinga catenaeformis*, most of which are evergreen (Table 2).

Ingeae

Three fossil species related to living species of *Chloroleucon*, *Enterolobium* and *Cedrelinga* were identified. Phytogeographically, this plant assemblage grows naturally in areas of South America where tropical and subtropical species converge, mainly in Paraguay and Brazil (Aróstegui & Díaz, 1992; Freitas, Madeiros & Lima, 1992; Evans *et al.*, 2006; Idárraga-Piedrahita *et al.*, 2011). In Argentina, Ingeae are represented by 24 species belonging to seven genera. The group is limited to the rainforest areas, many of which are typically secondary forests on poorly drained or periodically flooded soils (Hoc, 1987; Nielsen, 1987). *Chloroleucon* has a Neotropical distribution, from Mexico to Argentina. Three species live in Argentina: *Chloroleucon chacoense* (Burkart) Barneby & Grimes and *C. foliolosum* (Benth.) Lewis are typical bushes of the Yungas phytogeographic province in north-western Argentina, whereas *Chloroleucon tenuiflorum*, a tree species, grows from the slopes of the Sub-Andean Forest District and through the Chaco phytogeographic province, covering the xerophilous woodlands of Bolivia, central to northern Argentina and Paraguay (Pensiero *et al.*, 2005; Zapater *et al.*, 2016).

Enterolobium contortisiliquum extends from 3° to 36° S in South America, from northern to south-western Brazil, southern Bolivia and the riparian woodlands of Paranaense and Yungas phytogeographic provinces in Argentina (Tortorelli, 1956; Mogni *et al.*, 2015). *Chloroleucon* and *Enterolobium* have a close phenological and phylogenetic relationship *sensu* Barneby & Grimes (1996); at the level of the secondary xylem, a close relationship is also evident (Fig. 10).

In the Neotropical region, *Cedrelinga catenaeformis* is well established and there are records in Amazonia up to elevations not exceeding 1000 m a.s.l. in Ecuador (Aróstegui & Díaz, 1992; Freitas *et al.*, 1992; Perez *et al.*, 2014). This tree species is dominant and has a wide range of ecological adaptation in very humid tropical and subtropical woodlands to dry woodlands (Linares, 1986; Spichiger *et al.*, 1989; Freitas *et al.*, 1992; Richter & Dallwitz, 2000; Evans *et al.*, 2006; López, 2014). To the extent of our knowledge, there is no record of this taxon in Argentina. The species of Ingeae presented in this paper correspond to the first record for the Late Pleistocene in south-eastern South America.

Mimoseae

Four fossil species related to Mimoseae were identified. The tribe is represented by > 40 genera and *c.* 880 species distributed in tropical areas of America, Africa and India. In north-eastern Argentina, there are five genera (*Anadenanthera*, *Parapiptadenia*, *Piptadenia*, *Microlobius* and *Prosopis* L.) (Fernandez-Pacella, 2015; LPWG, 2017).

Anadenanthera spp. are resistant to seasonal environments. The presence in Argentina from the Miocene shows its success to survive to date, despite tectonic and climatic events that occurred during the Neogene and Quaternary. *Anadenanthera* has a notable and old record in the Miocene

(Caccavari & Anzótegui, 1987; Barreda, 1989; Caccavari & Barreda, 1992; Mautino, 2009; Franco & Brea, 2013) with Mid-Holocene pollen records in the Esteros del Iberá wetland (Middle Paraná River Basin), Corrientes province (Fernandez-Pacella, 2015). This distribution extends like an arc in South America from north-eastern Brazil, eastern Paraguay to north-eastern Argentina, including the present study area (Cialdella, 2000). It also extends throughout the sub-Andean Ranges piedmont woodlands of south-western Bolivia and north-eastern Argentina, and along the dry inter-Andean valleys of Bolivia and Peru (Prado & Gibbs, 1993).

Microlobius foetidus subspp. *foetidus* and *paraguensis* (Benth.) Sousa & Andrade are two subspecies of the monotypic genus *Microlobius*. They are native to America and distributed from Mexico to Argentina (Sousa Sánchez & Andrade, 1992). In Brazil they form part of the flora of the Pantanal of Mato Grosso do Sul, whereas in Argentina they border the Paraguay River in the humid and dry woodlands of the Chaco Phytogeographic province (Tortorelli, 1956; Cabrera, 1976; Sousa Sánchez & Andrade, 1992). The fossil record shows its presence from the Miocene in north-eastern Argentina (Franco & Brea, 2011). *Microlobiusxylon parafoetidus* reveals the presence of the genus in the Late Pleistocene of the lower-middle Basin of the Uruguay River. Low tolerance of the taxon to extreme temperatures and humidity changes and competition from other species of greater size is deduced.

All *Parapiptadenia* spp. are trees that occur in tropical and subtropical seasonally dry woodlands in South America. In Argentina, it grows in the Yungas and Paranaense phytogeographic provinces (Tortorelli, 1956; Cialdella, 2000; Forzza, 2010). In the El Palmar National Park fossiliferous locality (El Palmar Formation), *Piptadenioxylon chimeloi* Suguio & Mussa (Ramos *et al.*, 2012) was recovered. This fossil differs from *Parapiptadenioxylon pararigida*. The variations of features in the *Piptadenia* group could indicate a diversity of species already established in the Upper Pleistocene.

Pseudopiptadenia currently consists of *c*. 10 species, occurring in the Neotropical region (Jørgensen, Nee & Beck, 2014). They predominantly occur in damp woodlands that occur in the Atlantic and Amazon Forests, and only a few species, e.g. *Pseudopiptadenia bahiana* Lewis & M.P.Lima, grow in seasonally dry woodlands in the Caatinga. *Pseudopiptadenioxylon* (this work) corresponds to the first record of *Pseudopiptadenia* in Argentina. We consider that the genus grew successfully at lower latitudes in the Late Pleistocene, due to a non-seasonal or more stable climate than the present one. Overall, *Parapiptadenia* and *Pseudopiptadenia* are taxonomically related to *Microlobius* (Sousa Sánchez & Andrade, 1992; Simon *et al.*, 2016). This relationship is also reflected in wood anatomy. In fact, this behaviour groups these genera in PC 1 and 2 in the PCA analysis (Fig. 10, Appendix).

Among the plant assemblages, *Parapiptadenia*, *Microlobius*, *Anadenanthera*, *Chloroleucon* and *Enterolobium* form woodlands located in humid areas of Argentina, corresponding to the Paranaense, Yungas and Chaco phytogeographic provinces (Cabrera, 1976; Cialdella, 2000), whereas *Cedrelinga* and *Pseudopiptadenia* occur in the tropical and subtropical belt of South America (Forzza, 2010; Jørgensen *et al.*, 2014; Perez *et al.*, 2014). On this basis, it is supposed that the fossil species association identified here prospered successfully down to lower latitudes, due to better weather conditions for the coexistence of this plant assemblages (see CA method, Fig. 9).

Eco-anatomical significance of fossil woods

We explored the availability of water and temperature in which the plant assemblages recover in the Arroyo Yuquerí fossiliferous locality based on the quantitative and qualitative features of wood (Tables 1, 2, Appendix, Fig. 10). Caesalpinioideae are diverse in species and are distributed in a wide range of environments (LPWG, 2017). These species tend to express some features when growing in a particular environment, mainly those features directly conditioned by water availability, temperature and photoperiod (Evans *et al.*, 2006). Each environmental condition generates features in wood anatomy. The growth rings are a consequence of periodic dormancy, a strategy that many trees use to withstand conditions including drought, cold or photoperiodic events, common in plants that grew in significant environment seasonality (Carlquist, 2001; Evans *et al.*, 2006). In this context, the analysed fossils have marginal axial parenchyma, which was recorded as growth rings in the descriptions presented here. Nevertheless, we noted that there is no discontinuity between early- and latewood and that porosity is diffuse in all specimens. Therefore, it can be concluded that species did not have stress events and that marginal axial parenchyma corresponds to a feature commonly expressed in this taxonomic group (Caesalpinioideae). As suggested by some authors (Hacke *et al.*, 2016; Pratt & Jacobsen, 2017), we consider that, rather than a climate marker, it is an evolutionary adaptation related to storage and, indirectly, to hydraulic efficiency. Further research on this is in progress.

Baas (1983) stressed that wood anatomical features have great phenotypic plasticity, which contributes to the observation of ecological trends. The effect of environmental factors on wood features promotes intra- and interspecific variations, mainly in vessels/

mm², the diameter of vessels, the wall thickness in fibres and height and width of rays. These are ecological adaptations, and they are also related to evolution (Barajas-Morales, 1985; Carlquist & Hoekman, 1985; Wilkins & Papassotiriou, 1989; Arnold & Mauseth, 1999; Noshiro & Baas, 2000; Aguilar-Rodríguez & Barajas-Morales, 2005; Novaes *et al.*, 2010; Montaño-Arias, Camargo-Ricalde & Grether, 2016). Vessel features, helical thickenings in vessel elements and growth rings are shaped by climate and water availability (Baas & Schweingruber, 1987; Woodcock & Ignas, 1994; Weimann *et al.*, 1998; Carlquist, 2001; Martínez-Cabrera & Cevallos-Ferriz, 2008; Hajek *et al.*, 2016). The fossil species analysed here had rather mesomorphic behaviour, according to some of the above-mentioned features. This is strongly reflected in the analysis of vulnerability (VI) and MIs of Carlquist (2001). VI for the fossil woods ranges from 7 to 19, and MI ranges between 592 and 1270 (see Table 1). Generally, modern tropical trees have high VI (≥ 3) (Allen, 2017; Burnham & Johnson, 2004) and MI values > 200 (Carlquist, 2001). High VI values suggest that the El Palmar Formation woods did not experience significant water stress. According to Baas *et al.* (2004), Ewers *et al.* (2007) and Wheeler & Baas (1993), taxa found in tropical woodlands often have features that provide less resistance to hydraulic flow, including large diameter vessels, a low vessels frequency and simple perforation plates. If we consider this, the set of fossils presented here are associated with tropical species. Regarding the cluster analysis, among the fossils with larger vessel diameters and more vessels/mm², *Enterolobiumoxylon vassalloae* (white cross 4) and *Cedrelinga paleocatenaeformis* (white cross 2) can be mentioned (Fig. 10). In the analysis of the components CP 1, the diameter of the vessels seems to be the feature that separates these taxa from *Chloroleucoxylon yukeriense* (white cross 3). However, *Chloroleucoxylon* showed a mesomorphic feature, a vessel diameter not larger than 100 µm. Furthermore, the smaller fibre diameter and the absence of gums or deposits in the vessels are features not shared with *Enterolobiumoxylon vassalloae* and *Cedrelinga paleocatenaeformis*, which is why they are separated in the analysis of the components (CP 1), with *Chloroleucoxylon yukeriense* expressing on the negative axis and *Cedrelinga paleocatenaeformis* and *Enterolobiumoxylon vassalloae* on the positive axis (Fig. 10).

Likewise, the narrow vessels and diffuse porosity are features of shrubs and evergreen tropical montane, evergreen temperate and many deciduous temperate trees according to Baas *et al.* (2004) and Olson *et al.* (2014). Trees growing in more stressful environments tend to have significantly smaller vessel diameters than trees growing in humid and warm sites (Wheeler & Baas, 1993; Fichtler & Worbes, 2012; Olson *et al.*, 2014). The samples analysed for this work have diffuse porosity, only *Chloroleucoxylon yuqueriensis* has somewhat narrow vessels, whereas the rest of the fossils have wide vessels, and its modern analogues or NLRs are evergreens or semi-deciduous trees found in subtropical and tropical woodlands in South America.

The wood anatomy of tropical species usually has aliform, confluent wide axial parenchyma with bands of more than three cells (Baas, 1983; Wheeler, Baas & Rodgers, 2007; Morris *et al.*, 2016), features that were observed in the fossils under study. Highly dense axial parenchyma has been correlated with higher conduction capacity because the axial parenchyma may help to prevent cavitation or repair vessels when embolisms occur (Zheng & Martínez-Cabrera, 2013; Morris *et al.*, 2016). The fossil species analysed here do not show significant amounts of axial parenchyma. There is a particular case in the NLR (*C. catenaeformis*) in which axial parenchyma is scarce, and which also has quite large vessels and a greater number of rays/mm; these particular features highlight this taxon and this is manifest in the CP 1. This species is located on the positive axis distant from modern species living in seasonal and dry environments (see white triangle 3, Fig. 10).

The closest modern and fossil species are *Parapiptadenia* spp. and *Parapiptadenioxylon* (black cross 6), clearly compatible with their wood attributes (Tortorelli, 1956; Evans *et al.*, 2006). Regarding the behaviour of *Anadenantheroxylon kurupaum* (black cross 1) and its NLR, it was observed that vessels/mm² are significantly higher in *Anadenanthera peregrina* (black diamond 2) than in *Anadenantheroxylon kurupaum*, and this is the main reason for their separation in CP 1. The qualitative features that they do not share are: (1) variations in rays: in *Anadenantheroxylon kurupaum* and *Anadenanthera colubrina* (black diamond 1) rays one to three cells in width predominate, whereas in *Anadenanthera peregrina* they are multiseriate; and (2) in the presence/absence of marginal and diffuse axial parenchyma in one or another species (see Fig. 10, Appendix; Tortorelli, 1956; Evans *et al.*, 2006).

The grouping of *Enterolobium* spp. with *Chloroleucon tenuiflorum* in CP 1 is related to their eco-anatomical features including vessels/mm². They currently share habitats in Chaco, Yungas and Paranaense phytogeographic provinces of Argentina (Cozzo, 1951; Tortorelli, 1956; Cabrera, 1976; Oyarzabal *et al.*, 2018). Additionally, seven modern species (*Geoffroea decorticans*, *Cadia purpurea*, *Prosopis kuntzei*, *P. alpaca*, *P. vinalillo*, *Samanea saman* and *Mimosa polyantha*) from environments with marked seasonality were added to the cluster analysis. In fact, the general features of vessels were the causes that

separate this group on the negative axis of PC 1 and PC 2, far from fossils and their NLR (Fig. 10).

This work suggests a partial differentiation in wood anatomy in Ingeae and Mimoseae. Since these species are in the same subfamily, they do not present extreme variations, and the results can be seen in Figure 10 and the Appendix.

The values in MI and VI, the presence of growth rings demarcated by axial parenchyma, the dominance of diffuse porosity and short vessel elements and the moderate vessel density reflect a palaeo-environment with temperatures and precipitation similar to those that at present dominate at low-latitudes in South America. According to the CA, this Arroyo Yuquerí paleoflora coexisted in an environment with optimal temperature ranges from 22 to 28 °C, and rainfalls between 1300 and 1500 mm/year (Fig. 9).

Finally, and based on the evergreen habits of NLRs of Ingeae and Mimoseae, the prevailing climate during some events of the Late Pleistocene in the upper-Middle Basin of the Uruguay River in north-eastern Argentina was probably humid subtropical to tropical. Considering the sedimentological context of the fossil woods studied and the absolute datings of the El Palmar Formation, tropical humid conditions are deduced. The upper outcropping part of this sedimentary unit would represent the warm substage MIS 5a (covering most of the last major interglacial period before the present: MIS 5; Upper Pleistocene), and it is probably extended to the MIS 7 (Mid-Pleistocene). The new data presented here for the El Palmar Formation agree with palaeoclimatic inferences obtained from stratigraphical and sedimentological data (Iriondo, 1980; Iriondo & Kröhling, 2008; Kröhling, 2009) and palaeobotanical results (Zucol *et al.*, 2005; Brea *et al.*, 2010; Patterer *et al.*, 2014, 2020; Ramos *et al.*, 2014, 2017a, b; Ramos, 2015), and contribute to the palaeodiversity knowledge of the Quaternary flora of South America. A broader sampling and an increase in the number of species to be analysed would enhance the resolution of this type of study. Far from assuming that wood anatomy contributes conclusively to the taxonomy and phylogeny of Fabaceae, this research aims to infer on the behaviour of anatomical traits in relationship to ecology and taxonomic affinities, also considering the scope and limitations of secondary xylem.

CONCLUSIONS

The Late Pleistocene fluvial belt of the Uruguay River, represented by the El Palmar Formation, had a rich woody flora of Caesalpinioideae (Fabaceae). Seven new taxa were identified for the El Palmar Formation in the Arroyo Yuquerí fossil locality, in the Middle Basin of the Uruguay River (north-eastern Argentina): *Parapiptadenioxylon pararigida*, *Pseudopiptadenioxylon uniseriatum*, *Microlobiusxylon parafoetidus*, *Anadenantheroxylon kurupaum* (Mimoseae) and *Chloroleucoxylon yukeriense*, *Enterolobiumoxylon vassalloae* and *Cedrelinga paleocatenaeformis* (Ingeae). From this study, we can draw the following conclusions. (1) The study of fossil woods plays a key role in understanding palaeofloristic data and in reconstructing palaeoclimate of south-eastern South America. (2) The NLR method suggests that mature and perennial woodland was present in the upper/Middle Basin of the Uruguay River during some events of the Pleistocene (MIS 5a and MIS7, according to absolute datings of the fossiliferous sedimentary unit). (3) Fossil woods related to *Microlobius* and *Anadenanthera* were part of the Late Pleistocene palaeoflora in north-eastern Argentina, but only *Anadenanthera* survived until today in this region. *Microlobius* is currently distributed in latitudes below 27°S in South America. (4) In some phases of the Late Pleistocene (more probably in the MIS 5a), the climate was more humid and warmer than today, and therefore it differed from the modern seasonal climate in the study area. Nonetheless, from previous geological, paleobotanical and palaeontological studies, it is known that in the Pleistocene–Holocene there were events where the thermal amplitude and drought periods intensified (e.g. MIS 2, MIS 4, Late Holocene). This presumably acted as a barrier that influenced the dispersal and distribution of plants. (5) The eco-anatomical preliminarily results suggest that although the qualitative features of the secondary xylem position us in the taxonomic categories of genus and family of the fossils identified here, the quantitative features are those that define a specific level. Besides, quantitative features express the environment in which individuals grew up and are ultimately the natural factors that trigger speciation by expressing new features preserved in their genetics.

ACKNOWLEDGEMENTS

We thank Cristina Vassallo de Cettour and Silvia Cettour of the Museo de Ciencias Naturales y Antropología (Concordia, Entre Ríos, Argentina). We also would like to thank Geol. M. Belén Thalmeier (CONICET, Argentina), who processed DEM STRM and satellite images and the prepared Figure 1, and Facundo Gregorutti (Argentina), for providing linguistic help. We express our thanks to three anonymous reviewers and the Editor for their valuable help in providing critical and constructive comments. Margarita Herman helped us with correcting the English. Agencia Nacional de Promoción Científica y Tecnológica. Fondo para la investigación Científica y

Tecnológica (FONCYT). PICT 2008 N° 0176 and PICT 2017 N° 1281.

DATA AVAILABILITY

The data underlying this article are available in the repository of the fossil specimens and microscope slides is the Laboratorio de Paleobotánica, CICYTTP (CONICET-Prov. ER-UADER), Diamante-Argentina, and can be accessed with the acronym used for woods specimens: CIDPALBO-MEG 119, CIDPALBO-MEG 123, CIDPALBO-MEG 120, CIDPALBO-MEG 122, CIDPALBOMEG 127, CIDPALBO-MEG 129, CIDPALBO-MEG 128, CIDPALBO-MEG 132, CIDPALBO-MEG 137, CIDPALBO-MEG 141, CIDPALBO-MEG 143.

CONFLICT OF INTERESTS

The authors declare that there is no conflict of interests regarding the publication of this paper.

REFERENCES

Ab´Sáber NA. 2000. The natural organization of Brazilian inter- and subtropical landscapes. *Revista do Instituto Geológico, Sao Paulo* **21:** 57–70.

Aguilar Rodríguez S, **Barajas Morales J. 2005.** Anatomía de la madera de especies arbóreas de un bosque mesófilo de montaña: un enfoque ecológico-evolutivo. *Boletín de laSociedad Botánica de México* **2:** 51–58.

Allen S. 2017. Reconstructing the local vegetation and seasonality of the lower Eocene blue rim site of southwestern Wyoming using fossil wood. *International Journal of Plant Sciences* **178:** 1–26.

APG IV. **2016.** An update of the Angiosperm Phylogeny Group classification for the orders and families of flowering plants: APG IV. *Botanical Journal of the Linnean Society*. **181:** 1–20.

Arambarri AM, **Monti C**, **Bayón N**, **Hernández M**, **Novoa MC**, **Colares M. 2012.** Ecoanatomía foliar de arbustos y árboles del distrito Chaqueño oriental de la Argentina. *Bonplandia* **21:** 5–26.

Arana MD, **Natale E**, **Ferretti N**, **Romano G**, **Oggero A**, **Martínez G**, **Posadas P**, **Morrone JJ. 2021.** *Esquema biogeográfico de la República Argentina. Opera Lilloana 56.* Tucumán: Fundación Miguel Lillo.

Arnold DH, **Mauseth JD. 1999.** Effects of environmental factors on development of wood. *American Journal of Botany* **86:** 367–371.

Aróstegui A, **Díaz M. 1992.** *Propagación de especies forestales nativas promisorias en Jenaro Herrera.* Iquitos: Instituto de Investigaciones de la Amazonía Peruana.

Baas P. 1983. Ecological patterns of xylem anatomy. In: Givnish TJ, ed. *On the economy of plant form and function. Proceedings of the Sixth Maria Moors Cabot Symposium. Evolutionary constraints on primary productivity: adaptive patterns of energy capture in plants.* Cambridge: Cambridge University Press, 327–352.

Baas P, **Ewers FW**, **Davis SD**, **Wheeler EA. 2004.** Evolution of xylem physiology. In: Hemsley AR, Poole I, eds. *The evolution of plant physiology*. London: Elsevier, 273–295.

Baas P, **Schweingruber F. 1987.** Ecological trends in the wood anatomy of trees, shrubs and climbers from Europe. *IAWA Bulletin* **8:** 245–274.

Baez J, **Crisafulli A. 2020.** Novelties in the xylotaphoflora from Chiquimil Formation (Miocene), Catamarca-Argentina. *Journal of South American Earth Sciences* **107:** 98–125.

Baldin T, **Marchiori JNC. 2014.** Wood anatomy of *Albizia inundata* (Mart.) Barneby & J.W. Grimes (Fabaceae). *Balduinia* **46:** 25–31.

Banks H, **Gasson P. 2000.** Pollen morphology and wood anatomy of the *Crudia* group (Leguminosae, Caesalpinioideae, Detarieae). *Botanical Journal of the Linnean Society* **134:** 19–59.

Barajas-Morales J. 1985. Wood structural differences between trees of two tropical forests in Mexico. *IAWA Bulletin* **6:** 355–364.

Baretta-Kuipers T. 1981. Wood anatomy of Leguminosae: its relevance to taxonomy. In: Polhill, RM, Raven PH, eds. *Advances in legume systematics, Part 1.* Kew: Royal Botanic Gardens, 677–705.

Barneby RC, **Grimes JW. 1996.** Silk tree, guanacaste, monkey's earring. A generic system for the synandrous Mimosaceae of the Americas. Part I, *Abarema*, *Albizia* and allies. *Memoirs of the New York Botanical Garden* **74:** 1–292.

Barreda V. 1989. *Palinología estratigráfica de las sedimentitas Terciarias del 'Patagoniano' en los alrededores de la ciudad de Comodoro Rivadavia, provincias de Chubut y Santa Cruz. Tesis doctoral*, Universidad Nacional de Buenos Aires.

Barros CF, **Callado CH. 1997.** Timbers of the Atlantic rainforest: wood anatomy of species from remnant forests in Rio de Janeiro State, Brazil. Jardim Botanico de Rio de Janeiro **1:** 1–46.

Benicio JRW, **Pires EF**, **Da Rosa AAS**, **Spiekermann R**, **Uhl D**, **Jasper A. 2016.** A new fossil Fabaceae wood from the Pleistocene Touro Passo Formation of Rio Grande do Sul, Brazil. *Fossil Imprint* **72:** 251–264.

Bolzón de Muniz G, **Nisgoski S**, **Lomelí-Ramírez M. 2010.** Anatomía y ultraestructura de la madera de tres especies de *Prosopis* (Leguminosae-Mimosoideae) del Parque Chaqueño seco, Argentina. *Madera y Bosques* **16:** 21–38.

Bossi J. 1969. *Geología del Uruguay. 2nd edn. Colección Ciencias 12*. Montevideo: Universidad de la República, Departamento de Publicaciones.

Brandoni D, **Ferrero B**, **Brunetto E. 2010.** *Mylodon darwini* Owen (Xenarthra, Mylodontinae) from the Late Pleistocene of Mesopotamia, Argentina, with remarks on individual variability, paleobiology, paleobiogeography, and paleoenvironment. *Journal of Vertebrate Paleontology* **30:** 1547–1558.

Brazier JD. 1958. The anatomy of some timbers formerly included in *Piptadenia*. *Tropical Woods* **100:** 46–64.

Brea M. 1998. *Ulminium mucilaginosum* n.sp. y *Ulminium artabeae* n.sp., dos leños fósiles de Lauraceae en sedimentos de la Formacion El Palmar, provincia de Entre Ríos, Argentina. *Ameghiniana* **35:** 193–204.

Brea M. 1999. Leños fósiles de Anacardiaceae y Mimosaceae de la Formación El Palmar (Pleistoceno superior), departamento de Concordia, provincia de Entre Ríos, Argentina. *Ameghiniana* **36:** 63–69.

Brea M, **Aceñolaza PG**, **Zucol AF. 2001.** Estudio paleoxilológico en la Formación Paraná, Entre Ríos, Argentina. *Asociación Paleontológica Argentina, Publicación Especial 8. XI Simposio Argentino de Paleobotánica y Palinología*, 7–17.

Brea M, **Zucol A. 2001a.** Estudios paleobotánicos del Parque Nacional El Palmar (Entre Ríos, Argentina): silicobiolitos en sedimentos continentales del Pleistoceno Superior. *Ameghiniana* **38:** 29R.

Brea M, **Zucol A. 2001b.** Maderas fósiles de Combretaceae de la Formación El Palmar (Pleistoceno), provincia de Entre Ríos, Argentina. *Ameghiniana* **38:** 499–417.

Brea M, **Zucol A. 2011.** The Paraná-Paraguay Basin: geological and paleoenviromental. In: Albert JS, Reis RE, eds. *Historical biogeography of Neotropical freshwater fishes*. Berkeley, Los Angeles, London: University of California Press, 69–87.

Brea M, **Zucol A**, **Patterer N. 2010.** Fossil woods from late Pleistocene sediments from the El Palmar Formation, Uruguay Basin, eastern Argentina. *Review of Palaeobotany and Palynology* **163:** 35–51.

Bruneau A, **Lewis GP**, **Herendeen PS**, **Schrire B**, **Mercure M. 2008.** *Biogeographic patterns in early-diverging clades of the Leguminosae.* 98–99, in Botany 2008. Botany without Borders. [Botanical Society of America, Abstracts].

Burnham RJ, **Johnson KR. 2004.** South American paleobotany and the origins of Neotropical rainforests. *Philosophical Transactions of the Royal Society B: Biological Sciences* **359:** 1595–1610.

Cabrera AL. 1976. Regiones fitogeográficas argentinas. En: Kugler WF, ed. *Enciclopedia argentina de agricultura y jardinería. Tomo 2. Fascículo 1.* Buenos Aires: Acme, 1–85.

Caccavari M, **Anzótegui L. 1987.** Polen de Mimosoideae (Leguminosae) de la Formación Ituzaingó, Plioceno Superior de Corrientes, Argentina. *IV Congreso Latinoamericano de Paleontología, Bolivia* **1:** 443–458.

Caccavari M, **Barreda V. 1992.** Mimosoideae (Leguminosae) occurrences in the Early Miocene of Patagonia (Argentina). *Palaeogeography, Palaeoclimatology, Palaeoecology* **94:** 243–252.

Carlquist S. 2001. *Comparative wood anatomy. Systematic, ecological, and evolutionary aspects of dicotyledon wood. Springer Series in Wood Science.* Berlin: Springer.

Carlquist S, **Hoekman DA. 1985.** Ecological wood anatomy of the woody southern Californian flora. *IAWA Bulletin* **6:** 319–347.

Cassens DL, **Miller RB. 1981.** Wood anatomy of the New World *Pithecellobium* (*sensu lato*). *Journal of the Arnold Arboretum* **62:** 1–44.

Castro M. 1994. *Maderas argentinas de Prosopis. Atlas anatómico*. Buenos Aires: República Argentina, Presidencia de la Nación, Secretaría General.

Cheng YM, **Yang XN**, **He ZF**, **Mao B**, **Yin YF. 2018.** Early Miocene angiosperm woods from Sihong in the Jiangsu Province, Eastern China. *IAWA Journal* **39:** 125–142.

Cialdella AM. 2000. Fabaceae. Mismosoideae. Mimoseae: *Anadenanthera*, *Piptadenia*, *Parapiptadenia*. *Flora Fanerogámica Argentina* **67:** 1–10.

Costa CG, **Rauber Coradin VT**, **Czarneski CM**, **Da Pereira BA. 1997.** Bark anatomy of arborescent Leguminosae of Cerrado and gallery forest of Central Brazil. *IAWA Journal* **18:** 385–399.

Costa Ribeiro ML, **Barros C. 2006.** Variação intraspecífica do lenho de *Pseudopiptadenia contorta* (DC.) G.P. Lewis & M.P. Lima (Leguminosae - Mimosoideae) de populações ocorrentes em dois remanescentes de Floresta Atlântica. *Acta Botanica Brasilica* **20:** 839–844.

Cozzo D. 1951. Anatomía del leño secundario de las leguminosas Mimosoideas y Cesalpinoideas argentinas silvestres y cultivadas. Instituto Nacional de Investigaciones de las Ciencias Naturales y Museo Argentino Bernardino Rivadavia*, Ciencias Botánicas* **2:** 63–146.

Da Silva LB, **De Assis Ribeiro Dos Santos F**, **Gasson P**, **Cutler D. 2011.** Estudo comparativo da madeira de *Mimosa ophthalmocentra* Mart. ex Benth. e *Mimosa tenuiflora* (Willd.) Poir. (Fabaceae-Mimosoideae) na caatinga nordestina. *Acta Botatica Brasilica* **25:** 301–314.

Detienne P, **Jacquet P. 1983.** *Atlas d'identification des bois de l'Amazonie et des regions voisines.* Nogent s/Marne: Centre Technique Forestier Tropical.

Espinoza de PN, **Melandri J. 2006.** *Anatomía de la madera de 68 especies de la subfamilia Caesalpinoideae (Leguminosae) en Venezuela*. Mérida: Consejo de Desarrollo Científico, Humanístico y Tecnológico. Universidad de Los Andes.

Evans JA, **Gasson PE**, **Lewis GP. 2006.** Wood anatomy of the Mimosoideae (Leguminosae). *IAWA Journal* **Supplement 5:** 1.

Ewers FW, **Ewers JM**, **Jacobsen AL**, **López-Portillo J. 2007.** Vessel redundancy: modeling safety in numbers. *IAWA Journal* **28:** 373–388.

Farr ER, Zijlstra G, eds. 1996. *Index nominum genericorum (Plantarum)*. Available at: http://botany.si.edu/ing/

Fernandez Pacella L. 2015. Registro fósil y distribución de *Anadenanthera* en Argentina desde el Mioceno hasta la actualidad. *Estudios Geológicos* **71:** 5–31.

Ferrero BS, **Brandoni D**, **Noriega J**, **Carlini A. 2007.** Mamíferos de la Formación El Palmar (Pleistoceno tardío) de la provincia de Entre Ríos, Argentina. *Revista del Museo Argentino de Ciencias Naturales* **9:** 109–117.

Ferrero BS, **Patterer N**, **Brunetto E**, **Ramos RS**, **Noriega J**, **Moya E**, **Peralta M**, **Zucol A**, **Franco M**, **Brea M. 2019.** El registro paleontológico del Pleistoceno de la provincia de Entre Ríos (Argentina). Suplemento Mioceno al Pleistoceno del centro y norte de Argentina. *Opera Lilloana* **52:** 490–519.

Fichtler E, **Worbes M. 2012.** Wood anatomical variables in tropical trees and their relation to site conditions and individual tree morphology. *IAWA Journal* **33:** 119–140.

Forzza RC. 2010. Lista de espécies Flora do Brasil Rio de Janeiro. Jardim Botânico do Rio de Janeiro. Available at: http://floradobrasil.jbrj.gov.br/2010

Franco MJ, **Brea M. 2011.** *Microlobiusxylon paranaensis* gen. nov. et sp. nov. (Fabaceae-Mimosoideae) from the Pliocene- Pleistocene of Ituzaingó Formation, Paraná Basin, Argentina. *Revista Brasileira de Paleontologia* **13:** 103–114.

Franco MJ, **Brea M. 2013.** Leños fósiles de Leguminosas de la Formación Ituzaingó, Entre Ríos, Argentina: implicancias paleoecológicas y paleobiogeográficas. *Ameghiniana* **50:** 167–191.

Freitas da Silva M, **Medeiros L**, **de Lima C. 1992.** Leguminosas da Amazônia brasileira - II *Cedrelinga* Ducke (Leg. Mimos.). *Boletim do Museu Paraense Emilio Goeldi. Serie Botanica* **8:** 143–156.

Gasson PE. 1994. Wood anatomy of the tribe Sophoreae and related Caesalpinioideae and Papilionoideae. In: Ferguson IK, Tucker S, eds. *Advances in legume systematics. Structural botany 6.* Kew: Royal Botanic Gardens, 165–203.

Gasson PE, **Trafford C**, **Matthews B. 2003.** Wood anatomy of Caesalpinioideae. In: Klitgaard BB, Bruneau A, eds. *Advances in legume systematics 10*. Kew: Royal Botanic Gardens, 63–93.

Gimenez AM. 2009. Anatomía de madera, corteza y anillos de crecimiento de *Geoffroea decorticans* (Gill., ex Hook. & Arn.) Burk. *Quebracho* **17:** 16–30.

González S, **Cadenazzi M. 2015.** Recolonización natural por bosque ribereño en margen izquierda del embalse de Salto Grande: identificación de especies pioneras. *Agrociencia Uruguay* **19:** 1–13.

Gower JC. 1975. Generalized procrustes analysis. *Psychometrika* **40:** 33–51.

Gregory M, **Poole I**, **Wheeler EA. 2009.** Fossil dicot wood names an annotated list with full bibliography. *IAWA Journal* **Supplement 6:** 1–226.

Guido A, **Márgico LL. 2011.** Composición florística y estructura del componente leñoso del bosque asociado al Río Queguay Grande (Paysandú, Uruguay). *Recursos Rurais* **7:** 59–65.

Guimarães R. 2009. *Anatomia do lenho de* Anadenanthera colubrina *em diferentes fitofisionomias da Floresta Atlântica no Estado do Rio de Janeiro: Ilha Grande e Itatiaia*. Rio de Janeiro: 44 f. Dissertação (Mestrado em Botânica) - Instituto de Pesquisas Jardim Botânico do Rio de Janeiro/Escola Nacional de Botânica Tropical, Rio de Janeiro.

Guleria JS. 1984. Leguminous woods from the Tertiary of District Kachchh, Gujarat, western India. *The Palaeobotanist* **31:** 238–254.

Hacke UG, **Spicer R**, **Schreiber SG**, **Plavcová L. 2016.** An ecophysiological and developmental perspective on variation in vessel diameter. *Plant, Cell & Environment* **40:** 831–845.

Hajek P, **Kurjak D**, **Von Wühlisch G**, **Delzon S**, **Schuldt B. 2016.** Intraspecific variation in wood anatomical, hydraulic, and foliar traits in ten European beech provenances differing in growth yield. *Frontiers in Plant Science* **15:** 791–804.

Herendeen PS. 2000. Structural evolution in Caesalpinioideae. In: Herendeen PS, Bruneau A, eds. *Advances in legume systematics 9*. Kew: Royal Botanic Gardens, 45–64.

Hoc PS. 1987. *La tribu Ingeae Benth. en la Argentina. Estudio taxonómico y palinológico*. Doctoral Thesis, Buenos Aires: Universidad de Buenos Aires.

Höhn A. 1999. Wood anatomy of selected West African species of Caesalpiniodeae and Mimosoideae (Leguminosae):A comparative study. *IAWA Journal*. **20:** 115–146.

IAWA Committee. **1989.** IAWA list of microscopic features for hardwood identification. *IAWA Bulletin* **10:** 219–332.

Idárraga-Piedrahita A, **Ortiz RDC**, **Callejas Posada R**, **Merello M. 2011.** *Flora de Antioquia. Catálogo de las plantas vasculares. Listado de las plantas vasculares del Departamento de Antioquia, Vol.* **2**. Bogotá: D´vinni S.A.

Infostat. 2016. *Grupo InfoStat, FCA*. Córdoba: Universidad Nacional de Córdoba.

Insidewood. **2004-onwards.** *Insidewood*. Available at: http://www.insidewood.lib.ncsu.edu/search [july 2018]

Iriondo MH. 1980. El Cuaternario de Entre Ríos. *Revista de la Asociación de Ciencias Naturales del Litoral* **11:** 125–141.

Iriondo MH, **Kröhling D. 2008.** *Cambios ambientales en la cuenca del Uruguay (desde el Presente hasta dos millones de años atrás)*. Santa Fe: Colección Ciencia y Técnica, Universidad Nacional del Litoral.

Jordan GJ. 1997. Contrasts between the climatic ranges of fossil and extant taxa: causes and consequences for paleoclimatic estimates. *Australian Journal of Botany* **45:** 465–474.

Jørgensen PM, Nee MH, Beck SG, eds. 2014. *Catálogo de las plantas vasculares de Bolivia.* St. Louis: Missouri Botanical Garden Press.

Judd WS, **Campbell CS**, **Kellogg EA**, **Stevens PF. 1999.** *Plant systematics: a phylogenetic approach.* Sunderland: Sinauer Associates.

Klitgård BB, **Lewis GP. 2010.** Neotropical Leguminosae (Mimosoideae). In: Milliken W, Klitgård B, Baracat A. 2009 onwards. *Neotropikey - interactive key and information resources for flowering plants of the Neotropics*. Available at: https://www.kew.org/science/our-science/projects/neotropikey

Kloster A, **Gnaedinger S**, **Adami-Rodrigues K**, **Urban C. 2015.** New record of Fabaceae fossil woods from the Solimões Formation (Miocene), Acre Basin, Amazon, Brazil. *Revista Brasileira de Paleontologia* **18:** 391–402.

Kribs DA. 1968. *Commercial foreign woods on the American market*. New York: Dover Publications.

Kröhling D. 2009. La Formación El Palmar, una unidad fluvial asignable al subestadio cálido EIO 5a (Pleistoceno Tardío) de la cuenca del río Uruguay. *Natura Neotropicalis* **40:** 61–86.

Kröhling D, **Brunetto E**, **Galina G**, **Zalazar MC**, **Iriondo M. 2014.** Planation surfaces on the Parana Basaltic Plateau, South America. In: Rabassa J, Ollier C, Doe R, eds. *Gondwana landscapes of southern South America. Earth system sciences, Vol.* **1**. Dordrecht: Springer Science and Business Media, 247–303.

León W. 2008. Anatomía de madera en 31 especies de la subfamilia Mimosoideae en Venezuela. *Revista Colombia Forestal* **11:** 113–135.

Lewis GP, **Schrire BD**, **Mackinder BA**, **Lock M. 2005.** *Legumes of the World.* Kew: Royal Botanic Gardens.

Lima RS, **Oliveira PL**, **Rodrigues L. 2009.** Anatomia do lenho de *Enterolobium contortisiliquum* (Vell.) Morong (Leguminosae-Mimosoideae) ocorrente em dois ambientes. *Revista Brasileira de Botânica* **32:** 361–374.

Linares C. 1986. *Rodales y huertos semilleros en bosques tropicales*. Tarapoto: IIAP.

López AL. 2014. Available at: http://cedinfor.lamolina.edu.pe/Articulos_RFP/Vol10_no1-2_80-81_(14)/vol10_art10.pdf [Accessed March 2017].

Louppe D, Oteng-Amoako AA, Brink M, eds. 2008. *Plant resources of tropical Africa. 7(1).* Wageningen: Prota. [Accessed 8 March 2019].

Lowe JJ, **Walker MJ. 2014.** *Reconstructing Quaternary environments*. Abingdon-on-Thames: Routledge.

LPWG. 2017. A new subfamily classification of the Leguminosae based on a taxonomically comprehensive phylogeny. *Taxon* **66:** 44–77.

Lutz AI. 1979. Maderas de angiospermas (Anacardiaceae y Leguminosae) del Plioceno de la provincia de Entre Ríos, Argentina. *Facena* **3:** 39–63.

Lutz AI. 1980. *Palmoxylon concordiense* n. sp. del Plioceno de la Provincia de Entre Ríos, República Argentina. II Congreso Argentino de Paleobotánica y Bioestratigrafía y I Congreso Latinoamericano de Paleontología. Buenos Aires. **3:** 129–140.

Lutz AI. 1984. *Palmoxylon yuqueriense* n. sp. del Plioceno de la Provincia de Entre Ríos, Argentina. III Congreso Argentino de Paleontología y Bioestratigrafía, Corrientes. *Actas* 197–207.

Lutz AI. 1986. Descripción morfoeanatómica del estípite de *Palmoxylon concordiense* Lutz del Plioceno de la provincia de Entre Ríos, Argentina. *Facena* **6:** 17–32.

Lutz AI. 1991. Descripción anatómica de *Mimosoxylon* sp. del Plioceno (Formación Ituzaingó) de la provincia de Corrientes, Argentina. *Revista de la Asociación de Ciencias Naturales del Litoral* **22:** 3–10.

Mainieri C, **Chimelo JP**, **Alfonso VA. 1983.** *Manual de identificação das principais madeiras comerciais brasileiras.* São Paulo: Companhia de Promoção de Pesquisa Científica e Technológica do Estado de São Paulo.

Marchiori JN, **de Muñiz GI. 1996.** Anatomia do xilema secundário de *Mimosa pilulifera* Benth. *Ciência Florestal* **6:** 65–75.

Martinez L. 2014. Fossil legume woods from the Late Miocene, Chiquimil Formation (Santa María Basin), Argentina. *Review of Palaeobotany and Palynology* **201:** 1–11.

Martínez RM, **Crisafulli A. 2018.** Maderas cenozoicas de Termas de Río Hondo, Santiago del Estero, Argentina. *Revista del Museo Argentino de Ciencias Naturales* **21:** 87–100.

Martínez-Cabrera HI, **Cevallos-Ferriz SRS. 2008.** Palaeoecology of the Miocene El Cien Formation (Mexico) as determined from wood anatomical characters. *Review of Palaeobotany and Palynology* **150:** 154–167.

Mattos PP, **Teixeira LL**, **Seitz RA**, **Salis SM**, **Botosso PC. 2003.** *Anatomia de madeiras do Pantanal Mato-Grossense (características microscópicas).* Columbo, Corumbá: Embrapa.

Mautino L. 2009. *Palinofloras de las Formaciones San José y Chiquimil (Mioceno Medio y Superior), Noroeste de Argentina*. *Tesis doctoral*, Universidad Nacional del Nordeste.

Mautino L, **Garralla S. 2021.** Primeros registros palinológicospara Sudamérica afines a Pontederia, Gleditsia y Parkinsonia en la Formación Palo Pintado, Mioceno de Salta, Argentina. *Publicación Electrónica de la Asociación Paleontológica Argentina* **21:** 1–17.

Metcalfe CR, **Chalk L. 1950.** Anatomy of Dicotyle-dons: Leaves, stem, and wood in relation toanatomy with notes on economic uses. Clarendon Press, Oxford, **2:** 502–511.

Miller RB. 2007. Fluorescent woods of the World. In: Flynn JH Jr, ed. *A guide to the more useful woods of the World.* Madison: Forest Products Society.

Miller R, **Détienne P. 2001.** *Major timber trees of Guyana. Wood anatomy*. Wageningen: Tropenbos Foundation.

Mogni V, **Oakley L**, **Maturo H**, **Galetti L**, **Prado D. 2015.** Biogeografía y florística de los bosques secos estacionales Neotropicales (Bsen). *Revista OKARA*: *Geografia em Debate* **9:** 275–296.

Montaño-Arias SA, **Camargo-Ricalde SL**, **Grether R. 2016.** Anatomía de la madera de tres especies de *Mimosa* (Leguminosae-Mimosoideae) distribuidas en México. *Madera y Bosques* **22:** 191–202.

Morris H, **Plavcová L**, **Cvecko P**, **Fichtler E**, **Gillingham MAF**, **Martínez-Cabrera HI**, **Mcglinn DJ. 2016.** A global analysis of parenchyma tissue fractions in secondary xylem of seed plants. *New Phytologist* **209:** 1553–1565.

Mosbrugger V. 1999. The nearest living relative method. In: Jones TP, Rowe NP, eds. *Fossil plants and spores modern techniques.* London: The Geological Society, 261–265.

Mosbrugger V, **Utescher T. 1997.** The coexistence approach method for quantitative reconstructions of Tertiary terrestrial palaeoclimate data using plant fossils. *Palaeogeography, Palaeoclimatology, Palaeoecology* **134:** 61–86.

Moya E, **Brea M. 2015.** Legume fossil woods from the arroyo Feliciano Formation (late Pleistocene, northeastern Argentina): paleobiogeographic implications. *Ameghiniana* **52:** 558–573.

Müller-Stoll WR, **Mädel E. 1967.** Die fossilen Leguminosen-Hölzer. Eine Revision der mit Leguminosen verglichenen fossilen Hölzer und Beschreibungen älterer und neuer Arten. *Paleontographica* **119:** 95–174.

Muñiz GIB, **Nisgoski S**, **França R**, **Schardosin F. 2012.** Anatomia comparativa da madeira e carvão de *Cedrelinga catenaeformis* Ducke e *Enterolobium schomburgkii* Benth. para fins de identificação. *Scientia Forestalis* **40:** 291–297.

Nielsen I. 1987. Tribe Ingeae. In: Polhill RM, Raven PH, eds. *Advances in legume systematics 1*. Kew: Royal Botanic Gardens, 173–190.

Noshiro S, **Baas P. 2000.** Latitudinal trends in wood anatomy within species and genera: case study in *Cornus s.l.* (Cornaceae). *American Journal of Botany* **87:** 1495–506.

Novaes FS, **Callado CH**, **Pereira-Moura MVL**, **Lima HRP. 2010.** Wood anatomy of *Mollinedia glabra* (Spreng.) Perkins (Monimiaceae) in two Restinga vegetation formations at Rio das Ostras, RJ, Brazil. *Anais da Academia Brasileira de Ciências* **82:** 915–924.

Olson ME, **Anfodillo T**, **Rosell JA**, **Petit G**, **Crivellaro A**, **Isnard S**, **León-Gómez C**, **Alvarado-Cárdenas LO**, **Castorena M. 2014.** Universal hydraulics of the flowering plants: vessel diameter scales with stem length across angiosperm lineages, habits and climates. *Ecology Letters* **17:** 988–997.

Oyarzabal M, **Clavijo J**, **Oakley L. 2018.** Unidades de vegetación de la Argentina. *Ecología Austral* **28:** 40–63.

Patterer NI, **Kröhling DM**, **Zucol AF. 2020.** Phytolith analysis in Quaternary fluvial deposits (El Palmar Formation-Late Pleistocene) of the Uruguay river valley, Entre Ríos province, Argentina. *Journal of South American Earth Sciences* **100:** 102542.

Patterer NI, **Zucol AF**, **Brea M. 2014.** Análisis fitolíticos del perfil sedimentario Los Loros, de la Formación El Palmar (Pleistoceno superior), en el Parque Nacional El Palmar, Entre Ríos, Argentina. *Acta Geologica Lilloana* **26:** 53–62.

Pearson R, **Brown H. 1932.** *Commercial timbers of India, I and II.* Calcutta: Government of India Publications Branch.

Pensiero JF, **Gutiérrez HF**, **Lucchetti AM**, **Exner E**, **Kern V**, **Brnich E**, **Oakley L**, **Prado D**, **Lewis JP. 2005.** *Flora vascular de la Pcia. de Santa Fe. Claves para el reconocimiento de las familias y géneros. Catálogo sistemático de especies*. Santa Fe: UNL.

Pérez AJ, **Hernández C**, **Romero-Saltos H**, **Valencia R. 2014.** *Árboles emblemáticos de Yasuní, Ecuador.* Chicago: Field Museum.

Pérez-Lara DK, **Estrada-Ruiz E**, **Castañeda Posadas C. 2021.** *Kingiodendron* and *Enterolobium* Eocene woods from the El Bosque formation, Chiapas, Mexico. *Journal of South American Earth Sciences* **111:** 103–477.

Pons D, **de Franceschi D. 2007.** Neogene woods from western Peruvian Amazon and palaeoenvironmental interpretation. *Bulletin of Geosciences* **82:** 343–354.

Póvoa De Mattos P. 2003. *Anatomia de madeiras do Pantanal Mato-Grossense (características microscópicas).* Columbo, Corumbá: Embrapa.

Prado DE, **Gibbs PE. 1993.** Patterns of species distributions in the dry seasonal forests of South America. *Annals of the Missouri Botanical Garden* **80:** 902–927.

Prakash U. 1973. Fossil woods from the Tertiary of Burma. *The Palaeobotanist* **20:** 48–70.

Prakash U, **Barghoorn ES. 1961.** Miocene fossil woods from the Colombia basalts of Central Washington. *Journal of the Arnold Arboretum* **42:** 165–203.

Pratt RB, **Jacobsen AL. 2017.** Conflicting demands on angiosperm xylem: tradeoffs among storage, transport and biomechanics. *Plant, Cell and Environment* **40:** 897–913.

Pujana RR, **Martínez LCA**, **Brea M. 2011.** El registro de maderas fósiles de Leguminosae de Sudamérica. *Revista del Museo Argentino de Ciencias Naturales* **3:** 183–194.

Pujana RR, **Martinez LCA**, **García Massini JL**, **Di Iorio O**, **Penas Steinhardt A. 2014.** Legume (Mimosoideae) fossil woods from the late Miocene (Salicas Formation) of northwestern Argentina; Sociedade Brasileira de Paleontologia; *Revista Brasileira de Paleontologia* **17:** 317–326.

Quirk RM, **Miller RB. 1985.** Vestured pits in the tribe Cassieae Bronn (Leguminosae). *IAWA Bulletin* **6:** 200–212.

Ramanujam CGK. 1960. Silicified woods from the Tertiary rocks of South India. *Palaeontographica* **106:** 99–140.

Ramos RS. 2014. Análisis paleoecológico preliminar de la flora de La Formación El Palmar (Pleistoceno Tardío), Entre Ríos, Argentina. *Acta Geologica Lilloana* **26:** 63–74.

Ramos RS. 2015. *Estudios xilológicos en el Pleistoceno superior de la Formación El Palmar, Provincia de Entre Ríos, Argentina*. Doctorial Thesis, en Ciencias Biologicas. Universidad Nacional de Córdoba.

Ramos RS, **Brea M**, **Kröhling DM. 2012.** Leños fósiles de la Formación El Palmar (Pleistoceno Tardío) en el parque Nacional El Palmar, Entre Ríos. Argent. *Ameghiniana* **49:** 606–622.

Ramos RS, **Brea M**, **Kröhling DM. 2015.** Primer registro de *Cryptocaryoxylon* Leisman, una Lauraceae de la Formación El Palmar (Pleistoceno tardío), Entre Ríos, Argentina. *Revista del Museo Argentino de Ciencias Naturales* **17:** 59–70.

Ramos RS, **Brea M**, **Kröhling DM. 2017a.** Malvaceous wood from the Late Pleistocene El Palmar Formation of northeastern Argentina. *Review of Palaeobotany and Palynology*. **246:** 232–241.

Ramos RS, **Brea M**, **Kröhling DM. 2017b.** Fossil woods of Detarioideae subfamily (Fabaceae) from El Palmar Formation (Late Pleistocene) in South America. *Journal of South American Earth Sciences* **79:** 202–214.

Ramos RS, **Brea M**, **Pardo R. 2014.** Fossil wood of *Peltophoroxylon* (Caesalpinioideae) from the El Palmar Formation (Late Pleistocene), Argentina. *IAWA Journal* **35:** 199–212.

Ramos RS, **Contreras S**, **Vezzosi R**, **Leon C**, **Tasso J. 2020.** Charred wood and plant microremains associated to *Neosclerocalyptus* sp. (Cingulata, Chlamyphoriidae, Glyptodontinae) from the Upper Pleistocene of austral Chaco, Argentina. *Quaternary International*. **556:** 60–74.

Richter H, **Dallwitz M. 2000 (onwards).** *Commercial timbers: descriptions, illustrations, identification, and information retrieval.* Available at: www.http//biodiversity.uno.edu/delta/

Scheel-Ybert R, **Gonçalves T. 2017.** *Primeiro atlas antracológico de espécies brasileiras - first anthracological atlas of Brazilian species*. Rio de Janeiro: Museu Nacional, Universidade Federal do Rio de Janeiro.

Schuster J. 1910. Ueber Nicolien und Nicolien ähnliche Holzer. Kungliga Svenska vetenskapsakademiens handlingar **45:** 1–18.

Selmeier A. 1973. Verkieselte Leguminosenhölzer aus obermiozänen Glimmersanden der südlichen Frankenalb. *Mitteilungen der Bayerischen Staatssammlung für Paläontologie und Historische Geologie* **13:** 183–197.

Shukla A, **Mehrotra RC**, **Guleria JS. 2013.** African elements (fossil woods) from the upper Cenozoic sediments of western India and their palaeoecological and phytogeographical significance. *Alcheringa* **37:** 1–18.

Silva A, **Blanco C**, **Lindorf H. 1989.** Anatomía de la madera de nueve leguminosas de Venezuela. *Acta Botanica Brasilica* **2:** 115–134.

Simon M, **Barea Pastore J**, **Sousa A**, **Borges L**, **Scalon VR**, **Ribeiro PG**, **Santos-Silva J**, **Castro Souza V**, **Quieroz LP. 2016.** Molecular phylogeny of *Stryphnodendron* (Mimosoideae, Leguminosae) and generic delimitations in the *Piptadenia* group. *International Journal of Plant Sciences* **177:** 44–59.

Sousa Sánchez M, **Andrade G. 1992.** Identidad de *Microlobius* y *Goldmania* (Leguminosae: Mimosoideae: Mimoseae) y nuevas combinaciones. *Anales del Instituto de Biología, Universidad Nacional Autónoma de México* **63:** 101–107.

Spichiger R, **Meroz J**, **Loizeau P**, **Stutz De Ortega L. 1989.** *Contribución a la flora de la Amazonía peruana; los árboles del arborétum Jenaro Herrera. Vol. 1. 1.* Geneva: Conservatoire et Jardins Botaniques de Genève & Organización Suiza para

el Desarrollo y la Cooperación, Instituto de Investigaciones de la Amazonía Peruana.

Stepanovaab AV, **Oskolskiabp AA**, **Tilneyab M**, **Van Wyka E. 2013.** Wood anatomy of the tribe Podalyrieae (Fabaceae, Papilionoideae): diversity and evolutionary trends. *South African Journal of Botany* **89:** 244–256.

Suguio K, **Mussa D. 1978.** Madeiras fósseis dos aluviões antigos do Rio Tietê, São Paulo. *Boletim IG, Instituto de Geociências da Universidade de São Paulo* **9:** 25–45.

Tomazello Filho M, **Peres Chimelo J**, **Vieitez Garcia P. 1983.** Madeiras de espécies florestais do Estado do Maranhão: II - caracterização anatômica. *IPEF* **23:** 29–36.

Tonni E. 1987. *Stegomastodon platensis* y la antigüedad de la Formación El Palmar en el Departamento Colon, E. Rios. Nota paleontológica. *Ameghiniana* **24:** 323–324.

Tortorelli L. 1956. *Maderas y bosques Argentinos*. Buenos Aires: Editorial Acme.

Ulibarri EA. 2008. Los géneros de Caesalpinioideae (Leguminosae) presentes en Sudamérica. *Darwiniana* **46:** 69–163.

Utescher T, **Bruch A**, **Erdei B**, **François L**, **Ivanov D**, **Jacques FM**, **Kern AK**, **Liu Y**, **Mosbrugger V**, **Spicer RA. 2014.** The coexistence approach—theoretical background and practical considerations of using plant fossils for climate quantification. *Palaeogeogography Palaeoclimatology Palaeoecology* **410:** 58–73.

Valderrama Freyre H. 1998. Anatomía comparativa del xilema del tronco y de la rama de *Cedrelinga catenaeformis* Ducke (Fabaceae). *Revista Folia Amazónica* **9:** 5–28.

Veroslavsky G, **Ubilla M. 2007.** A snapshot of the evolution of the Uruguay River (Del Plata Basin). The Salto depositional sequence (Pleistocene, Uruguay, South America). *Quaternary Science Reviews* **26:** 2913–2923.

Villagra P, **Roig F. 1997.** Wood structure of *Prosopis alpataco* and *P. argentina* growing under different edaphic conditions. *IAWA Journal* **18:** 37–51.

Weimann MC, **Wheeler EA**, **Manchester SR**, **Portier KM. 1998.** Dicotyledonous wood anatomical characters as predictors of climate. *Palaeogeography Palaeoclimatology Palaeoecology* **139:** 83–100.

WFO. **2020.** World flora online. Available at: http://www.worldfloraonline.org. Accessed on: 21 June 2020.

Wheeler EA. 2011. InsideWood: a web resource for hardwood anatomy. *IAWA Journal* **32:** 199–211.

Wheeler EA, **Baas P. 1992.** Fossil wood of the Leguminosae: a case study in xylem evolution and ecological anatomy. In: Herendeen PS, Dilcher DL, eds. *Advances in legume systematics 4. The fossil record*. Kew: Royal Botanic Gardens, 281–301.

Wheeler EA, **Baas P. 1993.** The potentials and limitations of dicotyledonous wood anatomy for climatic reconstructions. *Paleobiology* **19:** 487–498.

Wheeler EA, **Baas P**, **Rodgers S. 2007.** Variations in dicot wood anatomy: a global analysis based on the InsideWood database. *IAWA Journal* **28:** 229–258.

Wheeler E, **Gasson P**, **Baas P. 2020.** Using the InsideWood web site: potentials and pitfalls. *IAWA Journal* **41:** 412–462.

Wilkins AP, **Papassotiriou S. 1989.** Wood anatomical variation of *Acacia melanoxylon* in relation to latitude. *IAWA Bulletin* **10:** 201–207.

Woodcock DW, **Ignas CM. 1994.** Prevalence of wood characters in eastern North America: what characters are most promising for interpreting climates fron fossil wood? *American Journal of Botany* **82:** 1243–1251.

Woodcock DW, **Meyer HW**, **Prado Y. 2017.** The Piedra Chamana fossil woods (Eocene, Peru). *IAWA Journal* **38:** 313–365.

Yahana T, **Javadi F**, **Onoda Y**, **Paganucci de Queiroz L**, **Faith D**, **Prado D**, **Akasaka M**, **Kadoya T**, **Ishihama F**, **Davies S**, **Ferry Slik J**, **Yi T**, **Ma K**, **Bin C**, **Darnaedi D**, **Pennington R**, **Tuda M**, **Shimada M**, **Ito M**, **Egan A**, **Buerki S**, **Raes N**, **Kajita T**, **Vatanparast M**, **Mimura M**, **Tachida H**, **Iwasa Y**, **Smith G**, **Victor J**, **Nkonki T. 2013.** Global legume diversity assessment: concepts, key indicators, and strategies. *Taxon* **62:** 249–266.

Zapater MA, **Hoc PS**, **Flores CB**, **Mamani CM**, **Lozano EC**, **Gil MN**, **Suhring SS. 2016.** *Chloroleucon tenuiflorum* (Leguminosae, Ingeae): morphometry of fruits, seeds and seedlings, healthy and germinability. *Global Journal of Biology, Agriculture and Health Sciences* **5:** 95–106.

Zheng J, **Martínez-Cabrera HI. 2013.** Wood anatomical correlates with theoretical conductivity and wood density across China: evolutionary evidence of the functional differentiation of axial and radial parenchyma. *Annals of Botany* **112:** 927–935.

Zucol AF, **Brea M**, **Scopel A. 2005.** First record of fossil wood and phytolith assemblages of the Late Pleistocene in El Palmar National Park (Argentina). *Journal of South American Earth Sciences* **20:** 33–43.

Zuloaga FO, **Morrone ON**, **Belgrano MJ**, **Marticorena C**, **Marchesi E. 2008.** Catálogo de las plantas vasculares del Cono Sur. *Monographs in Systematic Botany from the Missouri Botanical Garden* **107:** 33–48.

SUPPORTING INFORMATION

Additional Supporting Information may be found in the online version of this article at the publisher's web-site:

Appendix. Statistical analyses, database. References: Vessel TD = tangential diameter, RD = radial diameter, PI = intervessel pits, vessel element = lenght, Rays, width = W, height = H; Fibres, diameter = Df, non-septate = 1, septate = 2; Axial parenchyma, present = 1, absent = 2, A = aliform, C = confluent, V = vasicentric, M = marginal, D = difusse, B = banded; Rays type, homocellular = 1, heretocellular = 2; Rays seriation, uniseriate 90% = 1, rays two to three cells wide = 2, rays one to five cells wide = 3, two cells wide 70% = 4; more of four cells wide = 5; Crystals present = 1, absent = 2; Growth ring, present = 1, absent = 2; Gums, present = 1, absent = 2; Storied structure, present = 1, absent = 2, rays irregularly storied = 3.